HHS Public Access

Author manuscript

Bioorg Med Chem. Author manuscript; available in PMC 2021 December 22.

Published in final edited form as:

Bioorg Med Chem. 2021 December 15; 52: 116504. doi:10.1016/j.bmc.2021.116504.

LipE guided discovery of isopropylphenyl pyridazines as pantothenate kinase modulators

Lalit Kumar Sharma[a,b,1], **Mi Kyung Yun**[c], **Chitra Subramanian**[b], **Rajendra Tangallapally**[a], **Suzanne Jackowski**[b], **Charles O. Rock**[b], **Stephen W. White**[c], **Richard E. Lee**[a,*]

[a]Department of Chemical Biology and Therapeutics, St. Jude Children's Research Hospital, 262 Danny Thomas PI, MS1000, Memphis, TN 38105, United States

[b]Department of Infectious Diseases, St. Jude Children's Research Hospital, United States

[c]Department of Structural Biology, St. Jude Children's Research Hospital, United States

Abstract

Pantothenate kinase (PANK) is the critical regulator of intracellular levels of coenzyme A and has emerged as an attractive target for treating neurological and metabolic disorders. This report describes the optimization, synthesis, and full structure–activity relationships of a new chemical series of pantothenate competitive PANK inhibitors. Potent drug-like molecules were obtained by optimizing a high throughput screening hit, using lipophilic ligand efficiency (LipE) derived from human PANK3 IC_{50} values to guide ligand development. X-ray crystal structures of PANK3 with index inhibitors from the optimization were determined to rationalize the emerging structure activity relationships. The analysis revealed a key bidentate hydrogen bonding interaction between pyridazine and R306′ as a major contributor to the LipE gain observed in the optimization. A tractable series of PANK3 modulators with nanomolar potency, excellent LipE values, desirable physicochemical properties, and a well-defined structural binding mode was produced from this study.

Keywords

Pantothenate Kinase; Lipophilic ligand efficiency; Pyridazine; Hit-to-lead

*Corresponding author. Richard.Lee@stjude.org (R.E. Lee).

[1]Current address: NextRNA Therapeutics, Cambridge, Massachusetts, United States.

Declaration of Competing Interest

The authors declare that they have no known competing financial interests or personal relationships that could have appeared to influence the work reported in this paper.

Appendix A. Supplementary material

Supporting information (SI) includes Fig. S1 - Electron densities of compounds **31**, **55**, **56** within their respective PANK3 ternary complexes, and Table S1 - Data collection and Refinement Statistics. Supplementary data to this article can be found online at https://doi.org/10.1016/j.bmc.2021.116504.

1. Introduction

Coenzyme A is an essential metabolic cofactor required for mitochondrial function, fatty acid, and folate metabolism.[1] Pantothenate Kinase (PANK) catalyzes the first and rate-limiting step in Coenzyme A biosynthesis, regulating intracellular concentrations of CoA.[1–2] Human cells express four closely related isoforms of PANKs (PANK1α, PANK1β, PANK2, and PANK3) encoded by three genes in tissue-dependent ratios.[3–5] PANK2 is the major isoform in neural cells, and disabling genetic lesions in the PANK2 gene result in a devastating neurological disorder – pantothenate kinase associated neurodegeneration (PKAN).[3,6,7] Recently, we have demonstrated that the loss of PANK2 function can be compensated for by pharmacological activation of PANK, as a novel strategy to treat PKAN.[8] We have also shown that pharmacological activation of PANK can be used as novel method to treat coenzyme A sequestration and improve mitochondrial function in mice with propionic acidemia.[9] Inhibition of PANK may also be therapeutically desirable in some instances, such as for the treatment of diabetes where *Pank1* gene deletion produces mild hypoglycemia in the fasted state in mice,[10] or as an antimicrobial drug discovery target due to kingdom-specific differences in PanK function and structure.[11–12]

Given the documented association of PANK with diseases like PKAN and other metabolic diseases, we aimed to develop chemical probes that target PANK and are capable of modulating CoA levels to assess the potential of such compounds as therapeutics to treat these disorders. We performed a high throughput screen towards this goal.[13] However, the most potent hits identified suffered from poor solubility and a flat structure–activity relationship in preliminary follow-up studies. In response, we adjusted our hit prioritization strategy by applying both molecular weight (<350) and lipophilic ligand efficiency (LipE > 2) restrictions to our original hit list, to identify initial leads with improved biophysical properties (Fig 1A).[14] This reanalysis identified piperazine urea compound **1** (Fig 1B), with promising potency (IC_{50} = 0.51 μM) against PANK3 and a reasonable ligand efficiency (LipE = 2.8), but limited solubility (1.4 μM). In a recent communication, we described the use of the preclinical lead, **57**, as a therapeutic to treat pantothenate kinase associated neurodegeneration and briefly described the rationale behind its development.[8] Here, we report the synthesis of the 58 new molecules and the structure–activity relationships (SAR) responsible for the advancement of screening hit **1** to lead **57**. Optimization was guided by PANK3 IC_{50}s and crystal structures of the PANK3•ATP•pantazine complexes, but advancement of individual molecules was primarily driven by the LipE score to ensure the development of biologically useful PANK3 probes.

2. Results and discussion

To optimize the potency of **1**, systematic structural modifications around the *t*-butyl phenyl aniline (ring A) (analogs **1**–**27**), urea linker (analogs **28**–**34**), nicotinonitrile (ring C) (analogs **35**–**61**) were performed (Fig. 1B). The optimization was guided by lipophilic ligand efficiency (LipE = pIC_{50} − CLogP) to balance potency and lipophilicity contributions of the modifications, thus allowing for clear comparison between molecules and prioritizing new enthalpic contributions.[14–15] In this study, optimization of piperazine (ring B) is not explored because it serves as a spacer element as described below.

All the synthesized analogs of compound **1** were ranked for PANK3 affinity using a pantothenate phosphorylation assay with radiometric detection, as previously described.[14] These compounds are orthosteric inhibitors in the PANK3 assay but act as allosteric activators that elevate CoA levels in cells in the presence of pantothenate, in this study the SAR is followed only in the context of orthosteric inhibition.[8]

2.1. Synthesis of target molecules

The general method for the synthesis of analogs of the A-ring (**1**–**24**) is depicted in Scheme 1. First, 1-Boc piperazine was coupled with 6-chloronicotinonitrile (**63**) utilizing a microwave assisted nucleophilic aromatic substitution. The resulting product was then treated with tri-fluoroacetic acid in dichloromethane to remove the boc-protecting group. Intermediate **64** was then reacted with commercially available isocyanates (or synthesized from corresponding amines) producing the required piperazine ureas derivatives (**1**–**27**) (Table 1 and Fig. 2).

The analogs (**28**–**32**) with different linkers are synthesized as shown in schemes 2, 3 and 4. HATU assisted coupling of 6-(piperazin-1-yl) nicotinonitrile (**64**) with acids (**65**–**69**) in the presence of diisopropylethylamine (DIPEA) as the base gave analogs **28**, **30**, **31**, **33**, and **34** (Scheme 2). The carbamate derivatives **29** and **61** were prepared from *tert*-butyl piperazine-1-carboxylate (Scheme 3). The treatment of **62** with 1,1′-carbonyldiimidazole, followed by reaction with 4-isopropylphenol led to carbamate **71**. The boc-deprotection and reaction with 6-chloronicotinonitrile or 6-chloropyridazine-3-carbonitrile afforded **29** and **61** respectively in good yields.

6-(4-(2-(4-isopropylphenyl)-2-oxoethyl)piperazin-1-yl)nico-tinonitrile (**32**) was synthesized by reaction of **64** with 2-bromo-1-(4-isopropylphenyl)ethan-1-one (**72**) in the presence of diisopropylethylamine in CH_2Cl_2 (Scheme 4).

The synthesis of nicotinonitrile (ring C) analogs (**49**–**59**) is depicted in Schemes 5 and 6. To obtain urea derivatives, we first reacted 1-isocyanato-4-isopropylbenzene (**73**) and **62** which provided a urea intermediated **74**. Next, a reaction between **74** and heteroaryl halides resulted in required products **49**, **50**, **52**, **54**, **56** and **58** (Scheme 5). The intermediate **76** was prepared by coupling of **62** with 2-(4-isopropylphenyl)acetic acid **(75)**. Finally, **51**, **53**, **55**, **57**, and **59** were synthesized by reaction of corresponding heteroaryl halides with intermediate **76**. 2-oxoacetyl analog **60** was synthesized according to the route of **57** in Scheme 6, using 2-(4-isopropylphenyl)-2-oxoacetic acid in place of **75**.

2.2. Structure-Activity relationship

2.2.1. Optimization of t-butyl aniline motif—We first explored the effect of aliphatic substitution at the 4-position of the aniline moiety as shown in Table 1. We observed a clear pattern of structural requirements in our homologous series (compounds **1**–**9**). Removal of the aliphatic substituent at the 4-position to obtain compound **2** resulted in a significant loss of PANK3 inhibitory activity (IC_{50} > 10 μM). This clearly showed the importance of an alkyl side chain at the 4-position of the aniline moiety. The most optimal groups at this position were branched chains such as *i*-propyl (**5**), *t*-butyl (**1**), and *i*-butyl (**7**) at the

4-position. Interestingly, ethyl (**3**) and *n*-butyl (**8**) did not show activity (up to 10 μM), which indicated that a small branched chain aliphatic group is preferred at the 4-position. Consistent with this observation, the bioisosteric replacement of i-propyl with Br (**14**) and CF_3 (**18**) produced inactive compounds. Also, replacement of the aliphatic side chain at the 4 position with more polar electron donating and electron withdrawing groups resulted in a significant reduction in potency (**10**–**13, 17**).

Replacing the aromatic aniline ring with hydrophobic aliphatic substituents (Fig. 2) led to a complete loss of activity (**19**–**23**). Similarly, replacing the aniline ring with other aromatic groups also proved to be detrimental to activity (**24**–**27**). Overall, our initial SAR exploration on the aniline side of the molecule demonstrated that a branched aliphatic group at the 4-position of the aniline ring is critical for interaction with the PANK3. Even though *i*-butyl and *t*-butyl (**7** and **1** respectively) at 4-position had similar potency compared to *i*–propyl (**5**), the increase in lipophilicity was not desirable, and *i*-propyl was therefore prioritized for further development based on its LipE score.

2.2.2. Optimization of urea linker—We next investigated the effect of replacing the urea linker. First, replacement of the urea bond with a truncated amide bond (**28**) resulted in complete loss of activity. The carbamate linker in compound **29** was as efficient as urea (**5**), which suggested that a hydrogen bond donor group (NH) at this position is not required for interaction with PANK3. This result was supported by the improved activity of **31** which contains acetamide linker. Our interpretation for the improved activity of **31** compared to **5** is that the urea bond has restricted bond rotation that is removed in the acetamide linker in compound **31**, thus allowing the molecule to adopt the appropriate orientation for maximum interaction with the PANK3. Importantly, when the position of the carbonyl group in the linker was changed (compound **32**), a loss of activity was observed. These data suggested the importance of a hydrogen bond acceptor adjacent to piperazine for maintaining the interactions with the PANK3.

The acetamide linker in compound **31** was clearly superior to other linkers (compare compounds **5**, **28**–**32**). However, we also recognized that the increase in potency in **31** relative to **5** came at the cost of an increase in lipophilicity. So, for further structural modification, we investigated both urea and acetamide linkers. We also synthesized compounds **33** and **34** that had cyclopropane and *t*-butyl at position R_3, respectively, and had comparable activity to **31**, consistent with the SAR discussed in the prior section. The use of the LipE metric again high-lighted that *i*-propyl at the R_3–position provides an excellent balance between lipophilicity and potency (compare **31**, **33** and **34**).

2.2.3. Optimization of nicotinonitrile motif—In parallel to our examination of the urea linker, a survey of various substitutions on the nicotinonitrile side chain of the molecule was conducted (Table 3). Analysis of the fourteen synthesized compounds reveals a number of clear trends. Replacement of the nitrile with hydrogen (compound **35**), methyl (compound **36**), and electron-donating group such as amine (compound **37**) result in substantial loss of activity against PANK3. However, electron withdrawing substituents at the 3-position proved to be significant for the activity of compounds against PANK3. Although the order of

potency was found to be nitro > bromo = chloro > nitrile > trifluoromethyl (compare **5** and **40**–**43**), we advanced the nitrile at the 3-positon because of its low molecular weight and low lipophilicity. Indeed, this decision was supported by the LipE metric because **5** was more "efficient". The nitro group was discarded because of the known toxicity associated with this functionality. Interestingly, compound **48** in which the 1-position pyridyl nitrogen atom has been removed, retains the activity illustrating that the nitrogen atom at the 1-position is dispensable. However, removing nitrogen had a detrimental effect on LipE, so this substitution was not advanced. Changing the position of nitrile in the ring was also tolerated with a slight preference to 4-position (**39**) relative to 5-position (**38**).

To increase the molecule's polarity and explore additional hydrogen-bonding interactions with PANK3, we surveyed the effects of incorporating an additional nitrogen atom into the nicotinonitrile ring (Table 4). We observed a slight increase in potency in the pyrimidine-containing analogs. The 2, 6 pyrimidines **49, 50, 51** were similarly active than 3,5 pyrimidines **52**, **53**, although direct 4-cyano-2,6-pyrimidine analogs analogs were not generated, with **53** demonstrating the best activity. Pyrazines (**54** and **55**) further increased inhibitory activity. These results suggest that the introduction of nitrogen adjacent to the nitrile is desirable. A major increase in potency was observed in compounds containing a pyridazine ring (e.g., **56**–**61**), subsequently described as pantazines. Most importantly, this 60-fold improvement in potency came with the improvement in lipophilicity (~1 log unit reduction in ClogP), and thus we also observed significantly improved LipE. Such a gain in LipE potency is indicative of additional hydrogen bonding interactions with the protein. The SAR for the X linker motif (Table 2) is further reinforced in this series, with acetamide **53** demonstrating its superior activity compared to direct urea isostere **52**. This pattern is repeated for the 4-cyano pyridazine analogs **56**, **57**, **60**, **61** with acetamide > urea > carbamate > alpha-keto linker substitutions.

2.2.4. Structure analysis of PanK3-inhibitor interactions—To understand the SAR that led to the tight binding of **57**, we selected three key closely related molecules and determined the crystal structures of their PANK3·AMPNP·Mg^{2+} complexes (Fig 3, Supplementary Fig S1, Supplementary Table S1). In increasing order of affinity, compounds were pyridine **31** (IC_{50} 60 nM), urea **56** (IC_{50} 4 nM), and chloropyrazine **55** (IC_{50} 1.8 nM). We recently reported the structure of the PANK3•AMPPNP•Mg^{2+}• PZ-2891 (**57**) complex (PDB ID 6B3V),[8] and all three compounds bind in the same location (Fig. 3A, B, C and D). The compounds occupy the pantothenate binding site extending into the PANK3 dimer interface and engage both PANK3 protomers in the dimer, with the two equivalent sites in the dimer both occupied. The heteroaryl C ring and a portion of the piperazine linker ring engage the dimer interface at Trp341′ (prime indicates residues from the opposite monomer) by pi-pi stacking interaction. The acetamide or urea linker and the piperazine ring together generate the required compound length to optimally engage the docking sites on the two monomers. The three compounds were selected to investigate the tight binding of **57**; the role of the linker, the positioning and number of nitrogen atoms in the heteroaryl C ring, and the 3-substituent to the heteroaryl ring.

Ring A largely occupies the pantothenate binding site adjacent to the catalytic Glu138 and the bound AMPPNP•Mg^{2+}, and packs into a hydrophobic cavity created by V250′, I253′, Y254′, Y258′, L263′, and A269′. These residues reside on a flexible flap that reaches across from the opposite monomer, and the isopropyl substituent optimally fits into this pocket (Fig. 4A). At this site, a branched alkyl 4- phenyl ring is favored in our analog series (see Table 1), with isopropyl proving to be the most desirable. This motif overlays the pantothenate *gem*-dimethyl group's binding position found in pantothenate bound structures, [16] explaining the specificity at this position (Fig 4A).

The preferred linker is an acetamide rather than urea, and this is most evident by comparing the activities **56** (urea) with **57** (acetamide) where this is the only difference. In both linkers, the carbonyl group forms hydrogen bond interactions with Arg207 (Fig. 3A, 3B, 3C, 3D), and the low activity of **32** where the carbonyl group is immediately adjacent to the phenyl ring and unable to engage Arg207 confirms the importance of this interaction. However, in the weaker binding **56**, the urea NH group surprisingly forms an additional hydrogen bond interaction with the main chain carbonyl oxygen of Val268′ (Fig. 3C, 4B). This would suggest a tighter binding compound, but closer inspection reveals that the pyridazine and piperazine rings do not perfectly superimpose (Fig. 4B) and piperazine ring of **56** is distorted from its preferred puckered conformation (Fig. 4C). We suggest that the positions and conformations of the pyridazine and piperazine rings are optimal in **57** and that the rigidity of the planar urea linker in **56** has lower affinity because it prevents the two rings from adopting an ideal conformation.

An aromatic stacking interaction with W341 governs the binding affinity of the heteroaryl ring C and a key hydrogen bonding interaction between the heteroatoms and R306′. The 2-pyridyl nitrogen **31** does not interact with R306′ and is the least active (Fig 3A, 4B). In pyrazine **55**, the nitrogen at the 3 position forms a hydrogen bonding interaction with a terminal guanidine in R306′ (Fig 3B). In pyridazines **56** and **57**, the paired nitrogen atoms at the 2 and 3 positions form strong bidentate hydrogen bonding interaction with the guanidine group (Fig. 3C, 3D, 4B). This aspect of the SAR is evident and explains why electron-withdrawing groups (CN, Cl, NO_2) are favored at the 4 position, as they help enhance this hydrogen bonding pattern. The 4-substitution chlorine **55** and nitrile **57** appear to generate equally potent molecules, and both occupy a cavity afforded by Gly302′ and bounded by Ala337′ and Leu338′

2.2.5. Evaluation of physical properties—Based on their single-digit nM potencies and high lipophilicity ligand efficiency (LipE > 6), we evaluated our top candidates (Pantazines) (**56**, **57**) for their physiochemical properties (Table 5). The characterization of the in vitro ADME properties showed that **57** has a modest solubility in PBS buffer (pH 7.4) of 23 μM, approximately 16 times higher than the recorded solubility for our hit compound **1** (1.4 μM).[8] **56** showed lower solubility (5.5 μM) relative to **57**. However, **56** displayed higher stability to mouse, rat, and human microsomes compared to **57**. Passive permeability was assessed using the PAMPA assay, and good permeability was observed (316×10^{-6} cm/s for **56** and 413×10^{-6} cm/s for **57**). Both the compounds (**56** and **57**) showed no sign

of degradation in mouse, rat, and human plasma ($T_{1/2}$ = >48 h). The microsomal stability in all animal species was superior for **56** over **57**, with **57** being rapidly degraded.

3. Conclusion

In summary, we report the rapid LipE-guided optimization of the initial hit **1** to lead **57**, as illustrated in Fig. 5. This approach produced potent PANK3 binders with significant improvements in LipE and solubility, overcoming problems encountered with prior attempts to follow-up the PANK3 HTS data set, which focused on simply optimizing the most potent HTS hits. The increased solubility enabled the X-ray structures of the inhibitors bound to the PANK3•AMPPNP•Mg^{2+}complex to be determined. The structures revealed the binding position and the crucial interactions between key molecules in the series and PANK3, rationalizing the emerging SAR and facilitating further design efforts. The LipE metric favors the prioritization of enthalpic-driven binding. The LipE guidance identified the pyridazine-R306′ bidentate hydrogen bonding interaction as a strong and highly favorable interaction. A crucial advantage of the LipE approach is that the Pantazine leads **56** and **57** are naturally selected as highly efficient ligands with desirable in vitro ADME properties. Based in part on this successful study, the clinical development of PANK modulators is ongoing. Our studies suggest that other dormant HTS screening data sets could be re-evaluated using this approach to identify new starting points more amenable to optimization.

4. Methods

4.1. General methods

Unless otherwise noted, all reactions were carried out in flame-dried glassware under a static nitrogen atmosphere with anhydrous solvent. Chemical reactions were monitored by the thin-layer chromatography (TLC) and the Waters ACQUITY-UPLC-MS-UV system. Microwave-assisted chemical reactions were carried out in the Biotage Initiator^{+}. All reagents were obtained from commercially available sources and used without purification. Purification was handled by reverse phase HPLC or Biotage Flash column chromatography system, with silica cartridges acquired from Biotage Inc. All final compounds were purified to > 95% purity indicated as averages of the total wave count (TWC) and the ELSD readings in LC/MS chromatogram (column: Acquity BEH C18). 1H and 13C spectra were recorded using 400 MHz, using $CDCl_3$ or DMSO as a solvent. The chemical shifts are reported in parts per million (ppm) relative to DMSO (δ 2.50 ppm for proton NMR and δ 39.50 ppm for carbon NMR). Coupling constants are reported in hertz (Hz). The following abbreviations are used to designate the multiplicities: s = singlet, d = doublet, t = triplet, q = quartet, m = multiplet.

Compound 1. *N*-(4-(*tert*-butyl)phenyl)-4-(5-cyanopyridin-2-yl) piperazine-1-carboxamide

^{1}H NMR (400 MHz, $CDCl_3$) δ 8.46 (dd, J = 2.4, 0.8 Hz, 1H), 7.69 (dd, J = 9.0, 2.3 Hz, 1H), 7.38−7.32 (m, 2H), 7.30 (d, J = 2.1 Hz, 2H), 6.63 (dd, J = 9.0, 0.9 Hz, 1H), 6.31 (s, 1H), 3.83 (m, 4H), 3.74−3.65 (m, 4H), 1.32 (s, 9H). ^{13}C NMR (101 MHz, $CDCl_3$) δ 155.21, 152.77, 146.72, 140.23, 135.95, 125.99, 120.16, 105.84, 97.27, 43.93, 43.28, 34.45, 31.54. LC-MS (m/z): $C_{21}H_{25}N_5O$ Exact Mass 363.21; 364.01 (M^{+}+1 observed).

Compound 2. 4-(5-cyanopyridin-2-yl)-***N***-phenylpiperazine-1-carboxamide

^{1}H NMR (400 MHz, $CDCl_3$) δ 8.43 (dd, J = 2.3, 0.7 Hz, 1H), 7.67 (dd, J = 9.0, 2.3 Hz, 1H), 7.41−7.34 (m, 2H), 7.31 (dd, J = 8.7, 7.1 Hz, 2H), 7.11−7.03 (m, 1H), 6.61 (d, J = 9.0 Hz, 1H), 6.33 (s, 1H), 3.82 (dd, J = 6.7, 4.1 Hz, 4H), 3.69 (dd, J = 6.7, 4.1 Hz, 4H). ^{13}C NMR (101 MHz, $CDCl_3$) δ 159.04, 154.83, 152.62, 140.10, 138.52, 129.02, 123.55, 120.05, 118.37, 105.70, 43.77, 43.12. LC-MS (*m*/*z*): $C_{17}H_{17}N_5O$ Exact Mass 307.1; 308.1 (M^++1 observed).

Compound 3. 4-(5-cyanopyridin-2-yl)-***N***-(4-ethylphenyl)piperazine-1-carboxamide

^{1}H NMR (400 MHz, $CDCl_3$) δ 8.43 (dd, J = 2.4, 0.9 Hz, 1H), 7.66 (dd, J = 9.0, 2.3 Hz, 1H), 7.27 (m, 2H), 7.14 (d, J = 8.3 Hz, 2H), 6.60 (d, J = 9.0 Hz, 1H), 6.28 (s, 1H), 3.81 (dd, J = 6.6, 4.1 Hz, 4H), 3.72−3.63 (m, 4H), 2.61 (q, J = 7.5 Hz, 2H), 1.27−1.15 (m, 3H). ^{13}C NMR (101 MHz, $CDCl_3$) δ 159.30, 155.32, 152.87, 140.33, 139.94, 136.30, 128.59, 120.67, 118.64, 105.94, 97.37, 44.03, 43.37, 31.19, 28.47, 15.93. LC-MS (*m*/*z*): $C_{19}H_{21}N_5O$ Exact Mass 335.2; 336.0 (M^++1 observed).

Compound 4. 4-(5-cyanopyridin-2-yl)-***N***-(4-pentylphenyl)piperazine-1-carboxamide

^{1}H NMR (400 MHz, $CDCl_3$) δ 8.43 (dd, J = 2.4, 0.8 Hz, 1H), 7.66 (dd, J = 9.0, 2.3 Hz, 1H), 7.23 (d, J = 12.6 Hz, 2H), 7.12 (dd, J = 8.1, 6.1 Hz, 2H), 6.60 (dd, J = 9.1, 0.9 Hz, 1H), 6.30 (s, 1H), 3.80 (dd, J = 6.5, 4.2 Hz, 4H), 3.70−3.63 (m, 4H), 2.56 (m, 2H), 1.57 (m, 2H), 1.31 (m, 4H), 0.88 (m, 3H). ^{13}C NMR (101 MHz, $CDCl_3$) δ 159.19, 155.22, 152.77, 140.23, 138.52, 136.16, 129.39, 129.04, 121.87, 120.47, 118.54, 105.84, 97.27, 43.93, 43.27, 35.40, 31.58, 31.35, 22.69, 14.19. LC-MS (*m*/*z*): $C_{22}H_{27}N_5O$ Exact Mass 377.2; 378.1 (M^++1 observed).

Compound 5. 4-(5-cyanopyridin-2-yl)-***N***-(4-isopropylphenyl)piperazine-1-carboxamide

^{1}H NMR (400 MHz, $CDCl_3$) δ 8.42 (dd, J = 2.4, 0.8 Hz, 1H), 7.64 (dd, J = 9.0, 2.3 Hz, 1H), 7.28 (m, 2H), 7.20−7.09 (m, 2H), 6.58 (dd, J = 9.0, 0.8 Hz, 1H), 6.46 (s, 1H), 3.83−3.72 (m, 4H), 3.69−3.61 (m, 4H), 2.86 (hept, J = 7.0 Hz, 1H), 1.22 (d, J = 6.9 Hz, 6H). ^{13}C NMR (101 MHz, $CDCl_3$) δ 159.17, 155.32, 152.73, 144.42, 140.16, 136.31, 126.99, 120.67, 118.57, 105.82, 97.12, 43.91, 43.25, 33.63, 24.18. LC-MS (*m*/*z*): $C_{20}H_{23}N_5O$ Exact Mass 349.2; 349.4 (M^++1 observed).

Compound 6. 4-(5-cyanopyridin-2-yl)-***N***-(2-isopropyl-6-methylphenyl)piperazine-1-carboxamide

^{1}H NMR (400 MHz, $CDCl_3$) δ 8.48−8.40 (m, 1H), 7.66 (m, 1H), 7.22−7.13 (m, 2H), 7.08 (m, 1H), 6.66−6.57 (m, 1H), 5.83 (s, 1H), 3.80 (dd, J = 6.7, 4.0 Hz, 4H), 3.68 (dd, J = 6.8, 3.9 Hz, 4H), 3.12 (m, 1H), 2.25 (s, 3H), 1.21 (d, J = 6.9, 0.9 Hz, 6H). ^{13}C NMR (101 MHz, $CDCl_3$) δ 159.25, 156.14, 152.77, 145.95, 140.21, 136.24, 133.49, 128.28, 127.58, 123.70, 118.56, 105.88, 97.21, 44.09, 43.61, 28.69, 23.68, 18.83. LC-MS (*m*/*z*): $C_{21}H_{25}N_5O$ Exact Mass 363.2; 363.9 (M^++1 observed).

Compound 7. ***N***-(4-(***sec***-butyl)phenyl)-4-(5-cyanopyridin-2-yl) piperazine-1-carboxamide

^{1}H NMR (400 MHz, $CDCl_3$) δ 8.43 (d, J = 2.3 Hz, 1H), 7.66 (dd, J = 8.9, 2.3 Hz, 1H), 7.27 (d, J = 1.9 Hz, 2H), 7.12 (d, J = 8.5 Hz, 2H), 6.60 (d, J = 9.0 Hz, 1H), 6.28 (s, 1H), 3.86−3.74 (m, 4H), 3.71−3.60 (m, 4H), 2.56 (m, 1H), 1.57 (m, 3H), 1.21 (d, J = 6.9 Hz, 2H), 0.81 (t, J = 7.3 Hz, 3H). ^{13}C NMR (101 MHz, $CDCl_3$) δ 159.19, 155.23, 152.77, 143.26, 140.23, 136.26, 127.69, 120.47, 118.54, 105.84, 97.26, 43.93, 43.27, 41.22, 31.33, 31.09, 22.05, 12.36. LC-MS (m/z): $C_{21}H_{25}N_5O$ Exact Mass 363.2; 364.1 (M^++1 observed).

Compound 8. ***N***-(4-butylphenyl)-4-(5-cyanopyridin-2-yl)piperazine-1-carboxamide

^{1}H NMR (400 MHz, $CDCl_3$) δ 8.43 (dd, J = 2.4, 0.8 Hz, 1H), 7.66 (dd, J = 9.0, 2.3 Hz, 1H), 7.24 (m, 2H), 7.11 (d, J = 8.2 Hz, 2H), 6.60 (d, J = 9.0 Hz, 1H), 6.27 (s, 1H), 3.81 (m, 4H), 3.75−3.62 (m, 4H), 2.56 (t, J = 7.7 Hz, 2H), 1.59 (m, 2H), 1.34 (h, J = 7.4 Hz, 2H), 0.91 (t, J = 7.3 Hz, 3H). ^{13}C NMR (101 MHz, $CDCl_3$) δ 159.20, 155.21, 152.77, 140.23, 138.48, 136.17, 129.05, 120.46, 118.54, 105.84, 100.13, 97.27, 43.93, 43.27, 36.52, 35.12, 33.83, 31.09, 22.43, 14.10. LC-MS (m/z): $C_{21}H_{25}N_5O$ Exact Mass 363.2; 364.2 (M^++1 observed).

Compound 9. ***N***-(4-butyl-2-methylphenyl)-4-(5-cyanopyridin-2-yl) piperazine-1-carboxamide

^{1}H NMR (400 MHz, $CDCl_3$) δ 8.43 (dd, J = 2.4, 0.8 Hz, 1H), 7.66 (dd, J = 9.0, 2.3 Hz, 1H), 7.43 (d, J = 8.1 Hz, 1H), 7.00 (m, 2H), 6.65−6.56 (m, 1H), 6.05 (s, 1H), 3.81 (dd, J = 6.6, 4.2 Hz, 4H), 3.72−3.61 (m, 4H), 2.60−2.49 (m, 2H), 2.23 (s, 3H), 1.58 (m, 2H), 1.43−1.27 (m, 2H), 0.91 (t, J = 7.3 Hz, 3H). ^{13}C NMR (101 MHz, $CDCl_3$) δ 159.21, 155.67, 152.77, 140.22, 139.63, 134.12, 130.69, 129.66, 126.90, 123.60, 118.54, 105.84, 97.24, 43.93, 43.37, 35.19, 33.83, 22.50, 18.03, 14.11. LC-MS (m/z): $C_{22}H_{27}N_5O$ Exact Mass 377.2; 378.1 (M^++1 observed).

Compound 10. 4-(5-cyanopyridin-2-yl)-***N***-(4-methoxyphenyl) piperazine-1-carboxamide

^{1}H NMR (400 MHz, $CDCl_3$) δ 8.43 (dd, J = 2.3, 0.8 Hz, 1H), 7.66 (dd, J = 9.0, 2.3 Hz, 1H), 7.27 (s, 4H), 7.25 (d, J = 2.3 Hz, 1H), 6.91−6.80 (m, 2H), 6.60 (dd, J = 9.0, 0.9 Hz, 1H), 6.24 (s, 1H), 3.80 (d, J = 6.6 Hz, 8H), 3.71−3.62 (m, 4H); ^{13}C NMR (101 MHz, $CDCl_3$) δ 159.20, 156.37, 155.53, 152.76, 140.22, 131.57, 122.75, 118.54, 114.37, 105.84, 97.25, 55.66, 43.93, 43.24; LC-MS (m/z): $C_{18}H_{19}N_5O_2$ Exact Mass 337.2; 338.2 (M^++1 observed).

Compound 11. 4-(5-cyanopyridin-2-yl)-***N***-(4-(trifluoromethoxy) phenyl)piperazine-1-carboxamide

^{1}H NMR (400 MHz, $CDCl_3$) δ 8.44 (dd, J = 2.4, 0.8 Hz, 1H), 7.67 (dd, J = 8.9, 2.3 Hz, 1H), 7.43−7.35 (m, 2H), 7.22−7.12 (m, 2H), 6.61 (dd, J = 9.0, 0.8 Hz, 1H), 6.38 (s, 1H), 3.88−3.77 (m, 4H), 3.75−3.63 (m, 4H). ^{13}C NMR (101 MHz, $CDCl_3$) δ 159.22, 154.80, 152.83, 140.36, 137.45, 122.01, 121.33, 118.54, 105.93, 97.51, 43.94, 43.31. LC-MS (m/z): $C_{18}H_{16}F_3N_5O_2$ Exact Mass 391.1; 391.9 (M^++1 observed).

Compound 12. 4-(5-cyanopyridin-2-yl)-***N***-(4-(dimethylamino) phenyl)piperazine-1-carboxamide

^{1}H NMR (400 MHz, $CDCl_3$) δ 8.43 (dd, J = 2.3, 0.8 Hz, 1H), 7.66 (dd, J = 9.0, 2.3 Hz, 1H), 7.23−7.14 (m, 2H), 6.76−6.63 (m, 2H), 6.59 (dd, J = 9.1, 0.8 Hz, 1H), 6.16 (s, 1H), 3.87−3.71 (m, 4H), 3.71−3.58 (m, 4H), 2.91 (s, 6H). ^{13}C NMR (101 MHz, $CDCl_3$) δ 159.23, 155.89, 152.77, 148.10, 140.19, 128.23, 123.08, 118.58, 113.45, 105.84, 97.16, 43.96, 43.27, 41.18. LC-MS (*m*/*z*): $C_{19}H_{22}N_6O$ Exact Mass 350.2; 351.1 (M^++1 observed).

Compound 13. ***N***-(4-acetylphenyl)-4-(5-cyanopyridin-2-yl)piperazine-1-carboxamide

^{1}H NMR (400 MHz, $CDCl_3$) δ 8.44 (dd, J = 2.3, 0.8 Hz, 1H), 7.96−7.89 (m, 2H), 7.68 (dd, J = 9.0, 2.3 Hz, 1H), 7.54−7.44 (m, 2H), 6.61 (dd, J = 9.0, 0.8 Hz, 1H), 6.58 (s, 1H), 3.84 (dd, J = 6.7, 4.0 Hz, 4H), 3.72 (dd, J = 6.7, 4.0 Hz, 4H), 2.57 (s, 3H). ^{13}C NMR (101 MHz, $CDCl_3$) δ 197.10, 159.12, 154.21, 152.76, 143.29, 140.32, 132.30, 130.08, 129.97, 118.80, 118.59, 105.87, 97.52, 43.86, 43.31, 26.57. LC-MS (*m*/*z*): $C_{19}H_{19}N_5O_2$ Exact Mass 349.1; 350.00 (M^++1 observed).

Compound 14. ***N***-(4-bromophenyl)-4-(5-cyanopyridin-2-yl)piperazine-1-carboxamide

^{1}H NMR (400 MHz, $CDCl_3$) δ 8.43 (dd, J = 2.4, 0.7 Hz, 1H), 7.67 (dd, J = 9.0, 2.3 Hz, 1H), 7.45−7.37 (m, 2H), 7.31−7.26 (m, 2H), 6.60 (d, J = 9.0 Hz, 1H), 6.33 (s, 1H), 3.85−3.77 (m, 4H), 3.74−3.64 (m, 4H). ^{13}C NMR (101 MHz, $CDCl_3$) δ 159.15, 154.63, 152.76, 140.28, 137.82, 132.07, 121.71, 118.47, 116.20, 105.86, 97.42, 43.86, 43.23. LC-MS (*m*/*z*): $C_{17}H_{16}BrN_5O$ Exact Mass 385.1; 388.1 (M^++1 observed).

Compound 15. ***N***-(4-chlorophenyl)-4-(5-cyanopyridin-2-yl)piperazine-1-carboxamide

^{1}H NMR (400 MHz, $CDCl_3$) δ 8.43 (dd, J = 2.3, 0.8 Hz, 1H), 7.67 (dd, J = 9.0, 2.4 Hz, 1H), 7.36−7.30 (m, 2H), 7.27 (d, J = 6.0 Hz, 2H), 6.60 (d, J = 9.0 Hz, 1H), 6.35 (s, 1H), 3.82 (dd, J = 6.7, 4.1 Hz, 4H), 3.68 (dd, J = 6.7, 4.0 Hz, 4H). ^{13}C NMR (101 MHz, $CDCl_3$) δ 159.15, 154.72, 152.76, 140.28, 137.30, 129.13, 128.70, 121.43, 118.49, 105.86, 97.41, 43.87, 43.23. LC-MS (*m*/*z*): $C_{17}H_{16}ClN_5O$ Exact Mass 341.1; 342.2 (M^++1 observed).

Compound 16. 4-(5-cyanopyridin-2-yl)-***N***-(3,4-dichlorophenyl) piperazine-1-carboxamide

^{1}H NMR (400 MHz, $CDCl_3$) δ 8.43 (d, J = 2.3 Hz, 1H), 7.67 (dd, J = 9.0, 2.4 Hz, 1H), 7.61 (d, J = 2.5 Hz, 1H), 7.35 (d, J = 8.7 Hz, 1H), 7.21 (dd, J = 8.7, 2.6 Hz, 1H), 6.61 (d, J = 9.0 Hz, 1H), 6.39 (s, 1H), 3.88−3.78 (m, 4H), 3.73−3.64 (m, 4H). ^{13}C NMR (101 MHz, $CDCl_3$) δ 159.11, 154.33, 152.75, 140.31, 138.29, 132.86, 130.56, 126.77, 121.73, 119.28, 118.46, 105.87, 97.48, 43.82, 43.22. LC-MS (*m*/*z*): $C_{17}H_{15}Cl_2N_5O$ Exact Mass 375.1; 376.1 (M^++1 observed).

Compound 17. ***N***-(4-cyanophenyl)-4-(5-cyanopyridin-2-yl)piperazine-1-carboxamide

^{1}H NMR (400 MHz, $CDCl_3$) δ 8.44 (d, J = 2.3 Hz, 1H), 7.68 (dd, J = 9.0, 2.3 Hz, 1H), 7.63−7.56 (m, 2H), 7.51 (d, J = 8.8 Hz, 2H), 6.69−6.51 (m, 2H), 3.83 (dd, J = 6.7, 4.0 Hz, 4H), 3.71 (dd, J = 6.8, 4.1 Hz, 4H). ^{13}C NMR (101 MHz, $CDCl_3$) δ 159.10, 153.90, 152.75, 143.02, 140.35, 133.41, 119.43, 119.12, 118.41, 106.28, 105.88, 97.60, 43.82, 43.30. LC-MS (*m*/*z*): $C_{18}H_{16}N_6O$ Exact Mass 332.1; 333.0 (M^++1 observed).

Compound 18. 4-(5-cyanopyridin-2-yl)-***N***-(4-(trifluoromethyl) phenyl)piperazine-1-carboxamide

^{1}H NMR (400 MHz, $CDCl_3$) δ 8.44 (dd, J = 2.3, 0.8 Hz, 1H), 7.68 (dd, J = 9.0, 2.3 Hz, 1H), 7.56 (d, J = 8.6 Hz, 2H), 7.50 (d, J = 8.6 Hz, 2H), 6.61 (dd, J = 9.0, 0.9 Hz, 1H), 6.52 (s, 1H), 3.83 (dd, J = 6.5, 4.2 Hz, 4H), 3.77−3.62 (m, 4H). ^{13}C NMR (101 MHz, $CDCl_3$) δ 159.13, 154.36, 152.76, 141.92, 140.31, 126.43, 126.39, 119.36, 119.16, 118.45, 105.87, 97.49, 43.85, 43.27. LC-MS (m/z): $C_{18}H_{16}F_3N_5O$ Exact Mass 375.1; 376.2 (M^++1 observed).

Compound 19. 4-(5-cyanopyridin-2-yl)-***N***-cyclohexylpiperazine-1-carboxamide

^{1}H NMR (400 MHz, $CDCl_3$) δ 8.41 (d, J = 2.3 Hz, 1H), 7.64 (dd, J = 9.0, 2.3 Hz, 1H), 6.57 (d, J = 9.0 Hz, 1H), 4.27 (d, J = 7.7 Hz, 1H), 3.79−3.71 (m, 4H), 3.66 (m, 1H), 3.57−3.48 (m, 4H), 2.06−1.89 (m, 2H), 1.71 (m, 2H), 1.62 (m, 2H), 1.46−1.30 (m, 2H), 1.12 (m, 2H). ^{13}C NMR (101 MHz, $CDCl_3$) δ 159.23, 156.91, 152.75, 140.13, 118.61, 105.80, 97.01, 49.71, 43.90, 42.89, 34.13, 25.77, 25.19. LC-MS (m/z): $C_{17}H_{23}N_5O$ Exact Mass 313.2; 314.1(M^++1 observed)

Compound 20. ***N***-(***tert***-butyl)-4-(5-cyanopyridin-2-yl)piperazine-1-carboxamide

^{1}H NMR (400 MHz, $CDCl_3$) δ 8.41 (d, J = 2.3 Hz, 1H), 7.64 (dd, J = 9.0, 2.4 Hz, 1H), 6.57 (d, J = 9.0 Hz, 1H), 4.30 (s, 1H), 3.80−3.69 (m, 4H), 3.55−3.44 (m, 4H), 1.37 (s, 9H). ^{13}C NMR (101 MHz, $CDCl_3$) δ 159.24, 156.82, 152.76, 140.13, 118.63, 105.80, 96.98, 51.19, 43.94, 42.92, 29.58. LC-MS (m/z): $C_{15}H_{21}N_5O$ Exact Mass 287.2; 288.1 (M^++1 observed).

Compound 21. 4-(5-cyanopyridin-2-yl)-***N***-octylpiperazine-1-carboxamide

^{1}H NMR (400 MHz, $CDCl_3$) δ 8.44 (m, 1H), 7.64 (dd, J = 9.0, 2.3 Hz, 1H), 6.58 (dd, J = 9.0, 0.8 Hz, 1H), 4.42 (s, 1H), 3.80−3.71 (m, 4H), 3.58−3.51 (m, 4H), 3.25 (m, 2H), 1.28 (m, 12H), 0.92−0.83 (m, 3H). ^{13}C NMR (101 MHz, $CDCl_3$) δ 159.24, 157.65, 152.76, 140.15, 118.59, 105.81, 97.07, 43.94, 42.96, 41.22, 31.96, 31.09, 30.41, 29.47, 29.38, 27.11, 22.80, 14.25. LC-MS (m/z): $C_{19}H_{29}N_5O$ Exact Mass 343.2; 344.2 (M^++1 observed).

Compound 22. 4-(5-cyanopyridin-2-yl)-***N***-isopropylpiperazine-1-carboxamide

^{1}H NMR (400 MHz, $CDCl_3$) δ 8.41 (m, 1H), 7.64 (m, 1H), 6.57 (dd, J = 9.1, 1.8 Hz, 1H), 4.21 (d, J = 7.5 Hz, 1H), 4.09−3.92 (m, 1H), 3.74 (m, 4H), 3.52 (m, 4H), 1.18 (d, J = 6.4 Hz, 6H). ^{13}C NMR (101 MHz, $CDCl_3$) δ 159.24, 156.95, 152.76, 140.14, 118.60, 105.81, 97.05, 43.92, 42.89, 23.63. LC-MS (m/z): $C_{14}H_{19}N_5O$ Exact Mass 273.2; 274.1 (M^++1 observed).

Compound 23. ***N***-((3S,5S,7S)-adamantan-1-yl)-4-(5-cyanopyridin-2-yl)piperazine-1-carboxamide

^{1}H NMR (400 MHz, $CDCl_3$) δ 8.41 (d, J = 2.3 Hz, 1H), 7.64 (dd, J = 9.0, 2.3 Hz, 1H), 6.57 (d, J = 9.0 Hz, 1H), 4.18 (s, 1H), 3.74 (m, 4H), 3.57−3.45 (m, 4H), 2.09 (m, 3H), 1.99 (m, 6H), 1.68 (m, 6H). ^{13}C NMR (101 MHz, $CDCl_3$) δ 159.24, 156.45, 152.76, 140.11, 118.63,

105.78, 96.96, 51.68, 43.93, 42.92, 42.53, 36.58, 29.74. LC-MS (*m*/*z*): : $C_{21}H_{27}N_5O$ Exact Mass 365.2; 366.4 (M^++1 observed).

Compound 24. 4-(5-cyanopyridin-2-yl)-***N***-(4-methylbenzyl)piperazine-1-carboxamide

^{1}H NMR (400 MHz, $CDCl_3$) δ 8.41 (dd, J = 2.4, 0.7 Hz, 1H), 7.64 (dd, J = 9.0, 2.4 Hz, 1H), 7.21 (d, J = 8.0 Hz, 2H), 7.15 (d, J = 7.9 Hz, 2H), 6.58 (d, J = 9.0 Hz, 1H), 4.66 (m, 1H), 4.41 (d, J = 5.4 Hz, 2H), 3.79−3.70 (m, 4H), 3.60−3.51 (m, 4H), 2.34 (s, 3H). ^{13}C NMR (101 MHz, $CDCl_3$) δ 157.52, 152.85, 140.27, 137.51, 136.25, 129.63, 128.16, 118.67, 105.92, 45.14, 44.03, 43.12, 31.19, 21.36. LC-MS (*m*/*z*): $C_{19}H_{21}N_5O$ Exact Mass 335.2; 336.1 (M^++1 observed).

Compound 25. 4-(5-cyanopyridin-2-yl)-***N***-(furan-2-ylmethyl)piperazine-1-carboxamide

^{1}H NMR (400 MHz, $CDCl_3$) δ 8.41 (dd, J = 2.4, 0.8 Hz, 1H), 7.64 (dd, J = 9.0, 2.3 Hz, 1H), 7.36 (dd, J = 1.9, 0.9 Hz, 1H), 6.58 (dd, J = 9.1, 0.8 Hz, 1H), 6.33 (dd, J = 3.2, 1.9 Hz, 1H), 6.27−6.21 (m, 1H), 4.77 (m, 1H), 4.45 (d, J = 5.4 Hz, 2H), 3.79−3.71 (m, 4H), 3.60−3.53 (m, 4H). ^{13}C NMR (101 MHz, $CDCl_3$) δ 159.30, 157.23, 152.85, 152.32, 142.40, 140.27, 118.66, 110.72, 107.63, 105.91, 97.24, 43.99, 43.07, 38.17, 31.19. LC-MS (*m*/*z*): $C_{16}H_{17}N_5O_2$ Exact Mass 311.1; 312.1 (M^++1 observed).

Compound 26. Preparation of 4-(5-cyanopyridin-2-yl)-*N*-(2,3-dihy-dro-1H-inden-5-yl)piperazine-1-carboxamide $_1$H NMR (400 MHz, $CDCl_3$) δ 8.43 (dd, J = 2.1, 1.2 Hz, 1H), 7.66 (ddd, J = 9.0, 2.3, 0.8 Hz, 1H), 7.29 (d, J = 1.8 Hz, 1H), 7.13 (d, J = 8.0 Hz, 1H), 7.05−6.99 (m, 1H), 6.60 (dd, J = 9.1, 0.9 Hz, 1H), 6.28 (s, 1H), 3.80 (m, 4H), 3.72−3.63 (m, 4H), 2.87 (m, 4H), 2.06 (p, J = 7.3 Hz, 2H). ^{13}C NMR (101 MHz, $CDCl_3$) δ 159.30, 155.48, 152.87, 145.50, 140.32, 139.94, 136.79, 124.70, 118.81, 118.65, 117.28, 105.94, 97.34, 44.04, 43.38, 33.26, 32.53, 25.90. LC-MS (*m*/*z*): $C_{20}H_{21}N_5O$ Exact Mass 347.2; 348.1 (M^++1 observed).

Compound 27. 4-(5-cyanopyridin-2-yl)-***N***-(3-isopropylisoxazol-5-yl)piperazine-1-carboxamide

^{1}H NMR (400 MHz, $CDCl_3$) δ 8.44 (dd, J = 2.3, 0.8 Hz, 1H), 7.68 (dd, J = 9.0, 2.3 Hz, 1H), 7.37 (s, 1H), 6.61 (dd, J = 8.9, 0.8 Hz, 1H), 6.10 (s, 1H), 3.91−3.76 (m, 4H), 3.76−3.60 (m, 4H), 2.98 (h, J = 6.9 Hz, 1H), 1.27 (d, J = 6.9 Hz, 6H). ^{13}C NMR (101 MHz, $CDCl_3$) δ 171.32, 161.11, 159.06, 152.75, 151.31, 140.37, 118.37, 105.88, 97.69, 85.55, 43.74, 43.30, 27.10, 21.68. LC-MS (*m*/*z*): $C_{17}H_{20}N_6O_2$ Exact Mass 340.2; 341.2 (M^++1 observed).

Compound 28. 6-(4-(4-isopropylbenzoyl)piperazin-1-yl) nicotinonitrile

^{1}H NMR (400 MHz, $CDCl_3$) δ 8.42 (dd, J = 2.3, 0.8 Hz, 1H), 7.66 (dd, J = 9.0, 2.3 Hz, 1H), 7.45−7.32 (m, 2H), 7.31−7.27 (m, 2H), 6.62 (dd, J = 9.0, 0.8 Hz, 1H), 3.73 (m, 8H), 2.94 (h, J = 6.9 Hz, 1H), 1.27 (d, J = 6.9 Hz, 6H). ^{13}C NMR (101 MHz, $CDCl_3$) δ 171.03, 159.34, 152.78, 151.43, 140.25, 132.67, 127.48, 126.84, 118.46, 106.01, 97.42, 44.67, 34.24, 23.97. LC-MS (*m*/*z*): $C_{20}H_{22}N_4$ Exact Mass 334.2; 335.1 (M^++1 observed).

Compound 29. 4-isopropylphenyl 4-(5-cyanopyridin-2-yl)piperazine-1-carboxylate

^{1}H NMR (400 MHz, $CDCl_3$) δ 8.44 (dd, J = 2.3, 0.8 Hz, 1H), 7.67 (dd, J = 9.0, 2.3 Hz, 1H), 7.25−7.18 (m, 2H), 7.08−6.99 (m, 2H), 6.64 (dd, J = 9.0, 0.9 Hz, 1H), 3.75 (m, 8H), 2.91 (hept, J = 7.0 Hz, 1H), 1.24 (d, J = 6.9 Hz, 6H). ^{13}C NMR (101 MHz, $CDCl_3$) δ 159.31, 154.06, 152.79, 149.16, 146.25, 140.27, 127.44, 121.43, 118.48, 106.00, 97.38, 44.23, 33.76, 24.21. LC-MS (m/z): $C_{20}H_{22}N_4O_2$ Exact Mass 350.2; 352.0 (M^++1 observed).

Compound 30. 6-(4-(2-hydroxy-2-(4-isopropylphenyl)acetyl)piperazin-1-yl)nicotinonitrile

^{1}H NMR (400 MHz, $CDCl_3$) δ 8.37 (dd, J = 2.3, 0.8 Hz, 1H), 7.62 (dd, J = 9.0, 2.3 Hz, 1H), 7.23 (m, 4H), 6.63−6.51 (m, 1H), 5.23 (d, J = 6.3 Hz, 1H), 4.62 (d, J = 6.3 Hz, 1H), 3.94 (m, 1H), 3.79 (m, 1H), 3.74−3.57 (m, 2H), 3.51 (m, 1H), 3.46−3.27 (m, 2H), 3.12−2.97 (m, 1H), 2.88 (h, J = 6.9 Hz, 1H), 1.22 (d, J = 6.9 Hz, 6H). ^{13}C NMR (101 MHz, $CDCl_3$) δ 171.61, 159.05, 152.70, 149.84, 140.27, 136.49, 127.51, 127.49, 118.32, 105.89, 97.59, 71.64, 44.19, 43.55, 42.38, 38.77, 34.01, 31.09, 24.02. LC-MS (m/z): $C_{21}H_{24}N_4O_2$ Exact Mass 364.2; 365.3 (M^++1 observed).

Compound 31. 6-(4-(2-(4-isopropylphenyl)acetyl)piperazin-1-yl) nicotinonitrile

^{1}H NMR (400 MHz, $CDCl_3$) δ 8.42 (d, J = 2.3 Hz, 1H), 7.65 (dd, J = 9.0, 2.4 Hz, 1H), 7.21 (s, 4H), 6.58 (d, J = 9.0 Hz, 1H), 3.78 (m, 4H), 3.66 (m, 2H), 3.59 (m, 4H), 2.97−2.86 (m, 1H), 1.25 (d, J = 6.9 Hz, 6H). ^{13}C NMR (101 MHz, $CDCl_3$) δ 170.20, 159.19, 152.73, 147.81, 140.19, 131.95, 128.59, 127.09, 118.46, 105.89, 97.28, 45.58, 44.42, 44.05, 41.26, 40.85, 33.86, 24.11. LC-MS (m/z): $C_{21}H_{24}N_4O$ Exact Mass 348.2; 350.3 (M^++1 observed).

Compound 32. 6-(4-(2-(4-isopropylphenyl)-2-oxoethyl)piperazin-1-yl)nicotinonitrile

^{1}H NMR (400 MHz, $CDCl_3$) δ 8.40 (d, J = 2.3 Hz, 1H), 7.98−7.89 (m, 2H), 7.61 (dt, J = 9.1, 1.8 Hz, 1H), 7.32 (d, J = 7.9 Hz, 2H), 6.60 (d, J = 9.0 Hz, 1H), 3.88 (s, 2H), 3.77 (t, J = 5.0 Hz, 4H), 2.97 (hept, J = 7.0 Hz, 1H), 2.72 (t, J = 5.0 Hz, 4H), 1.27 (d, J = 6.8 Hz, 6H). ^{13}C NMR (101 MHz, $CDCl_3$) δ 195.54, 159.43, 155.29, 152.83, 139.98, 133.82, 128.46, 126.91, 118.83, 105.85, 96.53, 63.98, 53.11, 44.46, 34.46, 23.79. LC-MS (m/z): $C_{21}H_{24}N_4O$ Exact Mass 348.2; 349.9 (M^++1 observed).

Compound 33. 6-(4-(2-(4-cyclopropylphenyl)acetyl)piperazin-1-yl) nicotinonitrile

^{1}H NMR (400 MHz, $CDCl_3$) δ 8.39 (dd, J = 2.3, 0.8 Hz, 1H), 7.62 (dd, J = 9.0, 2.3 Hz, 1H), 7.13 (d, J = 8.1 Hz, 2H), 7.02 (d, J = 8.1 Hz, 2H), 6.56 (dd, J = 9.0, 0.9 Hz, 1H), 3.75 (m, 4H), 3.62 (m, 2H), 3.55 (m, 4H), 1.86 (m, 1H), 1.02−0.87 (m, 2H), 0.72−0.58 (m, 2H). ^{13}C NMR (101 MHz, $CDCl_3$) δ 170.15, 159.19, 152.74, 143.00, 140.19, 131.59, 128.52, 126.32, 118.46, 105.90, 97.31, 45.57, 44.42, 44.06, 41.26, 40.91, 15.20, 9.39. LC-MS (m/z): $C_{21}H_{22}N_4O$ Exact Mass 346.2; 347.2 (M^++1 observed).

Compound 34. 6-(4-(2-(4-(***tert***-butyl)phenyl)acetyl)piperazin-1-yl) nicotinonitrile

^{1}H NMR (400 MHz, $CDCl_3$) δ 8.45−8.34 (m, 1H), 7.63 (dd, J = 9.0, 2.3 Hz, 1H), 7.38−7.31 (m, 2H), 7.18 (d, J = 8.3 Hz, 2H), 6.56 (d, J = 9.0 Hz, 1H), 3.76 (m, 4H), 3.63 (m, 2H), 3.57 (m, 4H), 1.30 (s, 9H). ^{13}C NMR (101 MHz, $CDCl_3$) δ 170.17, 159.20, 152.75, 140.20,

131.62, 128.35, 125.95, 118.46, 105.89, 100.13, 97.31, 44.45, 44.07, 41.26, 40.72, 34.62, 31.48, 31.09. LC-MS (*m*/*z*): $C_{22}H_{26}N_4O$ Exact Mass 362.2; 363.1 (M^++1 observed).

Compound 35. ***N***-(4-isopropylphenyl)-4-(pyridin-2-yl)piperazine-1-carboxamide

^{1}H NMR (400 MHz, $CDCl_3$) δ 8.21 (ddd, J = 4.9, 2.0, 0.9 Hz, 1H), 7.52 (ddd, J = 8.5, 7.2, 2.0 Hz, 1H), 7.31−7.27 (m, 2H), 7.19−7.13 (m, 2H), 6.71−6.62 (m, 2H), 6.30 (s, 1H), 3.65 (s, 8H), 2.87 (hept, J = 6.7 Hz, 1H), 1.23 (d, J = 6.9 Hz, 6H). ^{13}C NMR (101 MHz, $CDCl_3$) δ 159.14, 155.37, 148.14, 144.19, 137.82, 136.51, 127.00, 120.45, 113.91, 107.25, 44.88, 43.75, 33.66, 24.22. LC-MS (*m*/*z*): $C_{19}H_{24}N_4O$ Exact Mass 324.2; 325.0 (M^++1 observed).

Compound 36. ***N***-(4-isopropylphenyl)-4-(5-methylpyridin-2-yl) piperazine-1-carboxamide

^{1}H NMR (400 MHz, $CDCl_3$) δ 8.03 (d, J = 2.3 Hz, 1H), 7.36 (d, J = 8.9 Hz, 1H), 7.30−7.26 (m, 2H), 7.21−7.13 (m, 2H), 6.61 (d, J = 8.6 Hz, 1H), 6.32 (s, 1H), 3.64 (m, 4H), 3.59 (m, 4H), 2.87 (h, J = 7.0 Hz, 1H), 2.21 (s, 3H), 1.27−1.18 (m, 6H). ^{13}C NMR (101 MHz, $CDCl_3$) δ 155.38, 144.17, 136.52, 127.40, 126.99, 123.08, 120.45, 77.48, 77.36, 77.16, 76.84, 45.50, 43.80, 33.66, 24.22, 17.48. LC-MS (*m*/*z*): $C_{20}H_{26}N_4O$ Exact Mass 338.2; 339.1 (M^++1 observed).

Compound 37. 4-(5-aminopyridin-2-yl)-***N***-(4-isopropylphenyl) piperazine-1-carboxamide

^{1}H NMR (400 MHz, $CDCl_3$) δ 8.49 (s, 1H), 7.62 (d, J = 2.8 Hz, 1H), 7.40−7.30 (m, 2H), 7.15−7.05 (m, 2H), 6.94 (dd, J = 8.8, 2.9 Hz, 1H), 6.68 (d, J = 8.8 Hz, 1H), 4.61 (s, 2H), 3.58−3.47 (m, 4H), 3.31−3.19 (m, 4H), 2.80 (hept, J = 6.9 Hz, 1H), 1.16 (d, J = 6.9 Hz, 6H ^{13}C NMR (101 MHz, $CDCl_3$) δ 155.35, 152.18, 141.91, 138.18, 137.60, 133.41, 126.09, 124.63, 120.00, 108.90, 46.55, 43.62, 32.84, 24.13. LC-MS (*m*/*z*): $C_{19}H_{25}N_5O$ Exact Mass 339.2; 340.3 (M^++1 observed).

Compound 38. 4-(3-cyanopyridin-2-yl)-***N***-(4-isopropylphenyl) piperazine-1-carboxamide

^{1}H NMR (400 MHz, $CDCl_3$) δ 8.37 (dd, J = 4.8, 2.0 Hz, 1H), 7.81 (dd, J = 7.6, 2.0 Hz, 1H), 7.28 (m, 2H), 7.20−7.13 (m, 2H), 6.82 (dd, J = 7.7, 4.8 Hz, 1H), 6.29 (s, 1H), 3.85−3.75 (m, 4H), 3.72−3.62 (m, 4H), 2.88 (m, 1H), 1.23 (d, J = 6.9 Hz, 6H). ^{13}C NMR (101 MHz, $CDCl_3$) δ 160.70, 155.32, 152.03, 144.32, 143.98, 136.40, 127.03, 120.50, 114.83, 95.46, 47.83, 43.79, 33.67, 24.21. LC-MS (*m*/*z*): $C_{20}H_{23}N_5O$ Exact Mass 349.2; 350.1 (M^++1 observed).

Compound 39. 4-(4-cyanopyridin-2-yl)-***N***-(4-isopropylphenyl) piperazine-1-carboxamide

^{1}H NMR (400 MHz, $CDCl_3$) δ 8.34−8.24 (m, 1H), 7.30−7.26 (m, 2H), 7.22−7.12 (m, 2H), 6.81 (m, 2H), 6.28 (s, 1H), 3.77−3.69 (m, 4H), 3.69−3.61 (m, 4H), 2.87 (m, 1H), 1.23 (d, J = 6.9 Hz, 6H). ^{13}C NMR (101 MHz, $CDCl_3$) δ 158.59, 155.26, 149.53, 144.41, 136.32, 127.05, 121.83, 120.52, 117.45, 114.00, 108.85, 44.31, 43.45, 33.67, 24.21. LC-MS (*m*/*z*): $C_{20}H_{23}N_5O$ Exact Mass 349.2; 350.1 (M^++1 observed).

Compound 40. ***N***-(4-isopropylphenyl)-4-(5-nitropyridin-2-yl)piperazine-1-carboxamide

^{1}H NMR (400 MHz, $CDCl_3$) δ 9.06 (d, J = 2.8 Hz, 1H), 8.26 (dd, J = 9.5, 2.7 Hz, 1H), 7.31−7.26 (m, 2H), 7.21−7.12 (m, 2H), 6.57 (d, J = 9.5 Hz, 1H), 6.30 (s, 1H), 3.90 (m, 4H), 3.75−3.66 (m, 4H), 2.86 (h, J = 7.0 Hz, 1H), 1.23 (d, J = 6.9 Hz, 6H). ^{13}C NMR (101 MHz, $CDCl_3$) δ 160.32, 155.19, 146.45, 144.55, 136.19, 135.71, 133.39, 127.08, 120.58, 104.71, 44.28, 43.23, 33.67, 24.20. LC-MS (*m*/*z*): $C_{19}H_{23}N_5O_3$ Exact Mass 369.2; 370.1 (M^++1 observed).

Compound 41. *N*-(4-isopropylphenyl)-4-(5-(trifluoromethyl)pyridin-2-yl)piperazine-1-carboxamide ^{1}H NMR (400 MHz, $CDCl_3$) δ 8.45−8.39 (m, 1H), 7.67 (dd, J = 9.0, 2.5 Hz, 1H), 7.31−7.26 (m, 2H), 7.21−7.13 (m, 2H), 6.64 (d, J = 9.0 Hz, 1H), 6.30 (s, 1H), 3.82−3.73 (m, 4H), 3.71−3.60 (m, 4H), 2.87 (hept, J = 7.0 Hz, 1H), 1.23 (d, J = 6.9 Hz, 6H). ^{13}C NMR (101 MHz, $CDCl_3$) δ 160.10, 155.29, 145.89, 144.38, 136.34, 134.89, 127.04, 120.53, 105.72, 44.23, 43.43, 33.66, 24.20. LC-MS (*m*/*z*): $C_{20}H_{23}F_3N_4O$ Exact Mass 392.2; 394.2 (M^++1 observed).

Compound 42. 4-(5-bromopyridin-2-yl)-***N***-(4-isopropylphenyl) piperazine-1-carboxamide

^{1}H NMR (400 MHz, $CDCl_3$) δ 8.21 (d, J = 2.5 Hz, 1H), 7.57 (dd, J = 9.0, 2.5 Hz, 1H), 7.28 (d, J = 1.9 Hz, 2H), 7.16 (d, J = 8.4 Hz, 2H), 6.55 (d, J = 9.0 Hz, 1H), 6.27 (s, 1H), 3.63 (m, 8H), 2.87 (m, 1H), 1.23 (d, J = 6.9, 6H). ^{13}C NMR (101 MHz, $CDCl_3$) δ 157.60, 155.31, 148.70, 144.28, 140.08, 136.42, 127.02, 120.47, 108.51, 108.31, 44.82, 43.57, 33.66, 24.21. LC-MS (*m*/*z*): $C_{19}H_{23}BrN_4O$ Exact Mass: 404.11; 405.1 (M^++1 observed).

Compound 43. 4-(5-chloropyridin-2-yl)-***N***-(4-isopropylphenyl) piperazine-1-carboxamide

^{1}H NMR (400 MHz, $CDCl_3$) δ 8.13 (d, J = 2.6 Hz, 1H), 7.46 (dd, J = 9.0, 2.7 Hz, 1H), 7.28 (m, 2H), 7.21−7.12 (m, 2H), 6.59 (d, J = 9.0 Hz, 1H), 6.31 (s, 1H), 3.63 (m, 8H), 2.87 (h, J = 6.9 Hz, 1H), 1.22 (d, J = 6.9 Hz, 6H). ^{13}C NMR (101 MHz, $CDCl_3$) δ 157.36, 155.33, 146.40, 144.28, 137.53, 136.42, 127.01, 120.84, 120.49, 107.93, 44.96, 43.59, 33.66, 24.21. LC-MS (*m*/*z*): $C_{19}H_{23}ClN_4O$ Exact Mass 358.1; 359.1 (M^++1 observed).

Compound 44. 4-(4-acetylphenyl)-***N***-(4-isopropylphenyl)piperazine-1-carboxamide

^{1}H NMR (400 MHz, $CDCl_3$) δ 7.95−7.86 (m, 2H), 7.31−7.26 (m, 2H), 7.20−7.13 (m, 2H), 6.86 (m, 2H), 6.36 (s, 1H), 3.74−3.64 (m, 4H), 3.49−3.41 (m, 4H), 2.87 (m, 1H), 2.54 (s, 3H), 1.22 (d, J = 6.9 Hz, 6H). ^{13}C NMR (101 MHz, $CDCl_3$) δ 196.69, 155.29, 153.71, 144.40, 136.35, 130.60, 128.24, 127.31, 127.04, 120.56, 113.61, 47.12, 43.63, 33.66, 26.32, 24.20, 24.18. LC-MS (*m*/*z*): $C_{22}H_{27}N_3O_2$ Exact Mass 365.2; 366.3 (M^++1 observed).

Compound 45. 4-(4-fluorophenyl)-***N***-(4-isopropylphenyl)piperazine-1-carboxamide

^{1}H NMR (400 MHz, $CDCl_3$) δ 7.28 (m, 2H), 7.20−7.13 (m, 2H), 7.02−6.95 (m, 2H), 6.93−6.86 (m, 2H), 6.33 (s, 1H), 3.68−3.60 (m, 4H), 3.18−3.09 (m, 4H), 2.87 (hept, J = 6.8 Hz, 1H), 1.22 (d, J = 7.0 Hz, 6H). ^{13}C NMR (101 MHz, $CDCl_3$) δ 158.94, 156.56, 155.30, 147.80, 147.78, 144.23, 136.49, 127.01, 120.44, 118.70, 118.62, 115.97, 115.75, 50.46, 44.33, 33.66, 24.21. LC-MS (*m*/*z*): $C_{20}H_{24}FN_3O$ Exact Mass 341.2; 342.3 (M^++1 observed).

Compound 46. 4-(3-chlorophenyl)-***N***-(4-isopropylphenyl)piperazine-1-carboxamide

^{1}H NMR (400 MHz, $CDCl_3$) δ 7.27 (m, 2H), 7.23−7.12 (m, 3H), 6.92−6.83 (m, 2H), 6.79 (m, 1H), 6.35 (s, 1H), 3.73−3.56 (m, 4H), 3.31−3.16 (m, 4H), 2.87 (m, 1H), 1.22 (d, J = 6.9 Hz, 6H). ^{13}C NMR (101 MHz, $CDCl_3$) δ 155.31, 152.04, 144.30, 136.43, 135.21, 130.32, 127.28, 127.01, 120.52, 120.13, 116.32, 114.39, 48.78, 44.01, 33.65, 24.20. LC-MS (*m*/*z*): $C_{20}H_{24}ClN_3O$ Exact Mass 357.2; 358.2 (M^++1 observed).

Compound 47. 4-(3,4-dichlorophenyl)-*N*-(4-isopropylphenyl) piperazine-1-carboxamide ^{1}H NMR (400 MHz, $CDCl_3$) δ 7.37−7.26 (m, 2H), 7.17 (m, 2H), 7.08 (m, 1H), 6.85 (m, 1H), 6.70 (m 2H), 3.58 (m, 4H), 3.18−3.03 (m, 4H), 2.86 (m, 1H), 1.26−1.17 (m, 6H). ^{13}C NMR (101 MHz, $CDCl_3$) δ 155.58, 152.18, 144.28, 136.56, 135.55, 126.81, 126.78, 121.08, 119.27, 113.93, 47.94, 43.58, 33.53, 24.12. LC-MS (*m*/*z*): $C_{20}H_{23}Cl_2N_3O$ Exact Mass 391.1; 392.2 (M^++1 observed).

Compound 48. 4-(4-cyanophenyl)-***N***-(4-isopropylphenyl)piperazine-1-carboxamide

^{1}H NMR (400 MHz, $CDCl_3$) δ 7.56−7.50 (m, 2H), 7.28 (s, 2H), 7.17 (d, J = 8.5 Hz, 2H), 6.89−6.82 (m, 2H), 6.30 (s, 1H), 3.74−3.64 (m, 4H), 3.48−3.39 (m, 4H), 2.87 (hept, J = 7.0 Hz, 1H), 1.23 (d, J = 6.9 Hz, 6H); ^{13}C NMR (101 MHz, $CDCl_3$) δ 155.20, 152.96, 144.46, 136.29, 133.77, 127.06, 120.53, 119.97, 114.34, 101.07, 46.90, 43.53, 33.67, 24.20; LC-MS (*m*/*z*): C21H24N4O Exact Mass 348.2; 348.2 (M^++1 observed).

Compound 49. 4-(4-cyanopyrimidin-2-yl)-***N***-(4-isopropylphenyl) piperazine-1-carboxamide

^{1}H NMR (400 MHz, $CDCl_3$) δ 8.48 (d, J = 4.7 Hz, 1H), 7.27 (d, J = 6.4 Hz, 2H), 7.17 (d, J = 8.4 Hz, 2H), 6.81 (d, J = 4.7 Hz, 1H), 6.30 (s, 1H), 3.98−3.90 (m, 4H), 3.67−3.56 (m, 4H), 2.87 (m, 1H), 1.23 (d, J = 6.9 Hz, 6H). ^{13}C NMR (101 MHz, $CDCl_3$) δ 161.28, 159.93, 155.31, 144.39, 141.87, 136.35, 127.05, 120.52, 116.15, 112.71, 43.79, 43.49, 33.67, 24.21. LC-MS (*m*/*z*): $C_{19}H_{22}N_6O$ Exact Mass 350.2; 351.1 (M^++1 observed).

Compound 50. 4-(5-bromopyrimidin-2-yl)-***N***-(4-isopropylphenyl) piperazine-1-carboxamide

^{1}H NMR (400 MHz, $CDCl_3$) δ 8.32 (d, J = 0.7 Hz, 2H), 7.28 (d, J = 1.9 Hz, 2H), 7.16 (d, J = 8.5 Hz, 2H), 6.29 (s, 1H), 3.97−3.79 (m, 4H), 3.63−3.54 (m, 4H), 2.88 (m, 1H), 1.22 (d, J = 6.9 Hz, 6H). ^{13}C NMR (101 MHz, $CDCl_3$) δ 159.88, 158.14, 155.35, 144.29, 136.43, 127.02, 120.49, 106.57, 43.80, 43.71, 33.66, 24.21. LC-MS (*m*/*z*): $C_{18}H_{22}BrN_5O$ Exact Mass 403.1; 404.3 (M^++1 observed).

Compound 51. 1-(4-(4-chloropyrimidin-2-yl)piperazin-1-yl)-2-(4-isopropylphenyl)ethan-1-one ^{1}H NMR (400 MHz, $CDCl_3$) δ 8.15 (d, J = 5.4 Hz, 1H), 7.18 (s, 4H), 6.53 (d, J = 5.2 Hz, 1H), 3.80 (dd, J = 6.6, 4.1 Hz, 2H), 3.75 (s, 2H), 3.71 (dd, J = 6.7, 4.0 Hz, 2H), 3.63 (dd, J = 6.5, 3.9 Hz, 2H), 3.50 (t, J = 5.2 Hz, 2H), 2.88 (m, 1H), 1.23 (d, J = 7.0 Hz, 6H). ^{13}C NMR (101 MHz, $CDCl_3$) δ 170.11, 161.44, 161.41, 158.98, 147.70, 132.16, 128.58, 127.06,

109.86, 45.95, 43.82, 43.72, 41.67, 40.96, 33.86, 24.12. LC-MS (*m*/*z*): $C_{19}H_{23}ClN_4O$ Exact Mass: 360.2; 361.2 (M^++1 observed).

Compound 52. 4-(2-cyanopyrimidin-5-yl)-***N***-(4-isopropylphenyl) piperazine-1-carboxamide

^{1}H NMR (400 MHz, $CDCl_3$) δ 8.34 (s, 2H), 7.25 (m, 2H), 7.21−7.13 (m, 2H), 6.30 (s, 1H), 3.80−3.68 (m, 4H), 3.58−3.48 (m, 4H), 2.88 (m, 1H), 1.23 (d, J = 6.9 Hz, 6H). ^{13}C NMR (101 MHz, $CDCl_3$) δ 155.09, 144.77, 144.00, 142.06, 136.01, 133.95, 127.13, 120.66, 116.50, 111.36, 45.58, 43.17, 33.68, 24.19. LC-MS (*m*/*z*): $C_{19}H_{22}N_6O$ Exact Mass 350.2; 351.2 (M^++1 observed).

Compound 53. 5-(4-(2-(4-isopropylphenyl)acetyl)piperazin-1-yl) pyrimidine-2-carbonitrile ^{1}H NMR (500 MHz, $CDCl_3$) δ 8.21 (s, 2H), 7.16 − 7.07 (m, 4H), 3.78 (t, J = 5.4 Hz, 2H), 3.69 (s, 2H), 3.65 − 3.55 (m, 2H), 3.33 (t, J = 5.4 Hz, 2H), 3.13 (t, J = 5.3 Hz, 2H), 2.82 (p, J = 6.9 Hz, 1H), 1.16 (d, J = 6.9 Hz, 6H). ^{13}C NMR (126 MHz, $CDCl_3$) δ 169.94, 147.89, 143.94, 142.14, 133.88, 131.58, 128.41, 127.07, 116.33, 45.64, 44.92, 40.74, 40.71, 33.73, 23.98. LC-MS (*m*/*z*): $C_{20}H_{23}N_5O$ Exact Mass 349.2; 350.5 (M^++1 observed).

Compound 54. 4-(5-cyanopyrazin-2-yl)-***N***-(4-isopropylphenyl) piperazine-1-carboxamide

^{1}H NMR (400 MHz, $CDCl_3$) δ 8.37 (d, J = 1.5 Hz, 1H), 8.14 (d, J = 1.5 Hz, 1H), 7.27 (m, 2H), 7.17 (m, 2H), 6.28 (s, 1H), 3.87 (m, 4H), 3.70 (m, 4H), 2.88 (m, 1H), 1.23 (d, J = 6.9 Hz, 6H). ^{13}C NMR (101 MHz, $CDCl_3$) δ 155.25, 153.98, 147.35, 144.77, 136.21, 131.11, 127.21, 120.72, 117.37, 117.30, 43.76, 43.31, 33.78, 24.30. LC-MS (*m*/*z*): $C_{19}H_{22}N_6O$ Exact Mass 350.2; 351.3 (M^++1 observed).

Compound 55 1-(4-(5-chloropyrazin-2-yl)piperazin-1-yl)-2-(4-isopropylphenyl)ethan-1-one

^{1}H NMR (400 MHz, $CDCl_3$) δ 8.06 (d, J = 1.5 Hz, 1H), 7.82 (d, J = 1.4 Hz, 1H), 7.18 (s, 4H), 3.76 (m, 4H), 3.56 (m, 4H), 3.39 (m, 2H), 2.88 (hept, J = 6.9 Hz, 1H), 1.23 (d, J = 6.9 Hz, 6H);). ^{13}C NMR (101 MHz, $CDCl_3$) δ 170.15, 153.56, 147.86, 141.28, 137.08, 132.09, 129.37, 128.65, 127.16, 45.60, 44.80, 44.66, 41.28, 40.92, 33.93, 24.19; LC-MS (*m*/*z*): $C_{19}H_{23}ClN_4O$ Exact Mass 358.2; 359.3 (M^++1 observed)

Compound 56. 4-(6-cyanopyridazin-3-yl)-***N***-(4-isopropylphenyl) piperazine-1-carboxamide

^{1}H NMR (400 MHz, $CDCl_3$) δ 7.50 (d, J = 9.6 Hz, 1H), 7.27 (m, 2H), 7.22−7.12 (m, 2H), 6.85 (d, J = 9.6 Hz, 1H), 6.35 (s, 1H), 3.98−3.87 (m, 4H), 3.81−3.65 (m, 4H), 2.87 (hept, J = 6.9 Hz, 1H), 1.23 (d, J = 6.9 Hz, 6H). ^{13}C NMR (101 MHz, $CDCl_3$) δ 158.56, 155.18, 144.63, 130.97, 127.09, 120.63, 109.99, 43.96, 43.13, 33.67, 29.01, 24.20. LC-MS (*m*/*z*): $C_{19}H_{22}N_6O$ Exact Mass 350.2; 351.1 (M^++1 observed).

Compound 57. 6-(4-(2-(4-isopropylphenyl)acetyl)piperazin-1-yl) pyridazine-3-carbonitrile

^{1}H NMR (400 MHz, $CDCl_3$) δ 7.45 (d, J = 9.6 Hz, 1H), 7.19 (m, 4H), 6.81 (d, J = 9.6 Hz, 1H), 3.82 (m, 2H), 3.76 (s, 2H), 3.75−3.66 (m, 4H), 3.63 (m, 2H), 2.88 (m, 1H), 1.23 (d, J = 6.9 Hz, 6H). ^{13}C NMR (101 MHz, $CDCl_3$) δ 170.27, 158.54, 147.93, 131.79, 130.91,

130.02, 128.59, 127.16, 116.68, 110.05, 45.42, 44.54, 44.01, 41.12, 40.85, 33.87, 24.11. LC-MS (*m*/*z*): $C_{20}H_{23}N_5O$ Exact Mass 349.2; 350.2 (M^++1 observed).

Compound 58. 4-(6-chloropyridazin-3-yl)-***N***-(4-isopropylphenyl) piperazine-1-carboxamide

^{1}H NMR (400 MHz, $CDCl_3$) δ 7.27 (m, 2H), 7.20−7.11 (m, 2H), 6.91 (m, 2H), 6.31 (s, 1H), 3.76 (dd, *J* = 6.7, 3.8 Hz, 4H), 3.68 (dd, *J* = 6.7, 3.8 Hz, 4H), 2.87 (m, 1H), 1.23 (d, *J* = 6.9 Hz, 6H). ^{13}C NMR (101 MHz, $CDCl_3$) δ 158.89, 155.26, 147.55, 144.42, 136.29, 129.18, 127.05, 120.53, 115.35, 44.73, 43.38, 33.67, 31.10, 24.21. LC-MS (*m*/*z*): $C_{18}H_{22}ClN_5O$ Exact Mass 359.2; 360.0 (M^++1 observed).

Compound 59. 1-(4-(6-chloropyridazin-3-yl)piperazin-1-yl)-2-(4-isopropylphenyl)ethan-1-one

^{1}H NMR (400 MHz, $CDCl_3$) δ 7.31 (m, 3H), 7.26 (m, 2H), 6.95 (d, *J* = 9.5 Hz, 1H), 3.87 (m, 2H), 3.83 (s, 2H), 3.68 (m, 2H), 3.63 (m, 4H), 2.96 (m, 1H), 1.31 (d, *J* = 6.9 Hz, 6H). ^{13}C NMR (101 MHz, $CDCl_3$) δ 170.17, 158.92, 147.79, 147.63, 132.00, 129.12, 128.60, 127.09, 115.48, 45.52, 45.39, 44.78, 41.26, 40.80, 33.86, 24.12. LC-MS (*m*/*z*): $C_{19}H_{23}ClN_4O$ Exact Mass 358.2; 359.1 (M^++1 observed).

Compound 60. 6-(4-(2-(4-isopropylphenyl)-2-oxoacetyl)piperazin-1-yl)pyridazine-3-carbonitrile

^{1}H NMR (400 MHz, $CDCl_3$) δ 8.00−7.81 (m, 2H), 7.51 (d, *J* = 9.6 Hz, 1H), 7.43−7.34 (m, 2H), 6.89 (d, *J* = 9.6 Hz, 1H), 4.02−3.80 (m, 6H), 3.61−3.50 (m, 2H), 3.00 (hept, *J* = 7.0 Hz, 1H), 1.28 (d, *J* = 6.9 Hz, 6H). ^{13}C NMR (101 MHz, $CDCl_3$) δ 190.70, 165.97, 158.58, 157.39, 131.06, 130.93, 130.39, 130.23, 127.51, 116.56, 110.32, 45.33, 44.75, 44.46, 40.94, 34.68, 23.69. LC-MS (*m*/*z*): $C_{20}H_{21}N_5O_2$ Exact Mass 363.2; 363.7 (M^++1 observed).

Compound 61. 4-isopropylphenyl 4-(6-cyanopyridazin-3-yl)piperazine-1-carboxylate

^{1}H NMR (400 MHz, $CDCl_3$) δ 7.51 (d, *J* = 9.6 Hz, 1H), 7.25−7.19 (m, 2H), 7.07−7.01 (m, 2H), 6.88 (d, *J* = 9.6 Hz, 1H), 3.86 (m, 8H), 2.91 (m, 1H), 1.24 (d, *J* = 6.9 Hz, 6H). ^{13}C NMR (101 MHz, $CDCl_3$) δ 158.65, 154.01, 149.09, 146.35, 130.96, 130.07, 127.47, 121.39, 116.72, 110.12, 44.01, 33.76, 24.20. LC-MS (*m*/*z*): $C_{19}H_{21}N_5O_2$ Exact Mass 351.2; 351.8 (M^++1 observed).

4.2. Biochemical methods

4.2.1. Materials—Sources of supplies were: D-[1-^{14}C]pantothenate (specific activity, 55 mCi/mmol), American Radiolabeled Chemicals; Ni-NTA resin, Qiagen corporation; Whatman DE81 filter paper, Sigma; All other materials were reagent grade or better.

4.2.2. PANK activity assays—PANK activity assays were performed as described earlier using purified recombinant human PANK3 proteins.[17] Briefly, the reaction mixture contained 100 mM Tris-HCl, pH 7.5, 10 mM $MgCl_2$, 2.5 mM ATP, 45 mM D-[1-^{14}C]pantothenate (specific activity, 22.5 mCi/mmol) and 25 ng of PANK protein ±

0–0.1 μM pantazine or 0–10 μM pantazine. The appropriate range for the IC_{50} determination was selected based on an initial activity determination for each compound at 10 μM. Each assay was incubated at 37 °C and the reaction was stopped after 10 min by the addition of 4 ml 10% (v/v) acetic acid. The mixture was spotted onto a DE81 ion-exchange filter disk and analyzed by scintillation counting. Curves (6 point) were performed in duplicate, data were combined and fit to Morrison's quadratic equation[18] (GraphPad software, version 9.2.0) that accounts for the impact of enzyme inhibitor binding on the free concentration of inhibitor.

4.3. Structural biology methods

4.3.1. Crystallization and structure determination—PanK3 with two amino acids (DD) added to the carboxy-terminus was expressed, purified and crystallized as previously described.[16] Compounds **31**, **55** and **56** were dissolved in DMSO at 25 mM concentration. To obtain the three complex cocrystal structures, the crystals of the PanK3•AMPPNP•Mg^{2+}•pantothenate complex were soaked in a solution containing 0.2 M ammonium acetate, 0.1 M citrate, pH 5.6, 50 mM $MgCl_2$, 32% polyethylene glycol 4000, 10 mM AMPPNP (adenosine 5′-(β,γ-imido)triphosphate) and 1 mM of compound (final 4% DMSO) for one to two days. Soaked crystals were cryoprotected with 29% ethylene glycol and diffraction data were collected at the SER-CAT beam line 22-ID and 22-BM at the Advanced Photon Source, and processed using HKL2000.[19] The structures were solved by molecular replacement using the PANK3 structure (PDB ID: 5KPR) and the program PHASER.[20] The structures were refined and optimized using PHENIX and COOT, respectively.[21,22] The refined structures were validated using MolProbity.[23] The atomic coordinates and structure factors have been deposited in the Protein Data Bank. The PDB codes, and the data collection and refinement statistics are presented in Supplementary Table S1. All structures were rendered with PyMOL (version 2.3.0, Schrödinger, LLC).

4.4. In vitro ADME profiling

The in vitro ADME values (Solubility, PAMPA and Caco 2 permeability, Plasma Protein binding, metabolic and plasma stability) was deterimined as previously reported.[24,25]

5. Notes

The authors retain patent rights pertaining to compounds in this series.

Supplementary Material

Refer to Web version on PubMed Central for supplementary material.

Acknowledgment

This work was supported by National Institutes of Health, United States grant GM034496 (CR) Cancer Center Support Grant CA21765, and by the American Lebanese Syrian Associated Charities (ALSAC). The content is solely the responsibility of the authors and does not necessarily represent the official views of the National Institute of Health or other funding agencies. We thank the support of the St Jude Chemical Biology and Therapeutics department Analytical Technologies Center for the generation of the in vitro ADME testing data, and Katie Creed for the performance of the enzyme assays.

Abbreviations:

PANK	Pantothenate kinase
CoA	coenzyme A
PKAN	PanK-associated neurodegeneration
SAR	structure-activity relationship
LipE	lipophilic ligand efficiency

References

[1]. Leonardi R, Zhang Y, Rock C, Jackowski S. Coenzyme A: back in action. Prog Lipid Res. 2005;44(2–3):125–153. [PubMed: 15893380]

[2]. Jackowski S, Rock CO. Regulation of coenzyme A biosynthesis. J Bacteriol. 1981; 148(3):926–932. [PubMed: 6796563]

[3]. Zhou B, Westaway SK, Levinson B, Johnson MA, Gitschier J, Hayflick SJ. A novel pantothenate kinase gene (PANK2) is defective in Hallervorden-Spatz syndrome. Nat Genet. 2001;28(4):345–349. [PubMed: 11479594]

[4]. Zhang Y-M, Rock CO, Jackowski S. Feedback regulation of murine pantothenate kinase 3 by coenzyme A and coenzyme A thioesters. J Biol Chem. 2005;280(38): 32594–32601. [PubMed: 16040613]

[5]. Rock CO, Karim MA, Zhang Y-M, Jackowski S. The murine pantothenate kinase (Pank1) gene encodes two differentially regulated pantothenate kinase isozymes. Gene. 2002;291(1–2):35–43. [PubMed: 12095677]

[6]. Johnson MA, Kuo YM, Westaway SK, et al. Mitochondrial localization of human PANK2 and hypotheses of secondary iron accumulation in pantothenate kinase-associated neurodegeneration. Ann N Y Acad Sci. 2004;1012:282–298. [PubMed: 15105273]

[7]. Kotzbauer PT, Truax AC, Trojanowski JQ, Lee VM. Altered neuronal mitochondrial coenzyme A synthesis in neurodegeneration with brain iron accumulation caused by abnormal processing, stability, and catalytic activity of mutant pantothenate kinase 2. J Neurosci: The Official J Soc Neurosci. 2005;25(3):689–698.

[8]. Sharma LK, Subramanian C, Yun M-K, et al. A therapeutic approach to pantothenate kinase associated neurodegeneration. Nat Commun. 2018;9(1). 10.1038/s41467-018-06703-2.

[9]. Subramanian C, Frank MW, Tangallapally R, et al. Pantothenate kinase activation relieves coenzyme A sequestration and improves mitochondrial function in mice with propionic acidemia. Sci Transl Med. 2021;13(611). 10.1126/scitranslmed.abf5965.

[10]. Garcia M, Leonardi R, Zhang YM, Rehg JE, Jackowski S. Germline deletion of pantothenate kinases 1 and 2 reveals the key roles for CoA in postnatal metabolism. PLoS One. 2012;7(7):e40871. [PubMed: 22815849]

[11]. Barnard L, Mostert KJ, van Otterlo WAL, Strauss E. Developing Pantetheinase-Resistant Pantothenamide Antibacterials: Structural Modification Impacts on PanK Interaction and Mode of Action. Acs Infect Dis. 2018;4(5):736–743. [PubMed: 29332383]

[12]. Spry C, Macuamule C, Lin Z, Virga KG, Lee RE, Strauss E, Saliba KJ. Pantothenamides are potent, on-target inhibitors of Plasmodium falciparum growth when serum pantetheinase is inactivated. PLoS One. 2013;8(2):e54974. [PubMed: 23405100]

[13]. Sharma LK, Leonardi R, Lin W, et al. A high-throughput screen reveals new small-molecule activators and inhibitors of pantothenate kinases. J Med Chem. 2015;58 (3):1563–1568. [PubMed: 25569308]

[14]. Shultz MD. The thermodynamic basis for the use of lipophilic efficiency (LipE) in enthalpic optimizations. Bioorg Med Chem Lett. 2013;23(21):5992–6000. [PubMed: 24054120]

[15]. Johnson TW, Gallego RA, Edwards MP. Lipophilic Efficiency as an Important Metric in Drug Design. J Med Chem. 2018;61(15):6401–6420. [PubMed: 29589935]

[16]. Subramanian C, Yun M-K, Yao J, et al. Allosteric Regulation of Mammalian Pantothenate Kinase. J Biol Chem. 2016;291(42):22302–22314. [PubMed: 27555321]

[17]. Hong BS, Senisterra G, Rabeh WM, et al. Crystal structures of human pantothenate kinases. Insights into allosteric regulation and mutations linked to a neurodegeneration disorder. J Biol Chem. 2007;282(38):27984–27993. [PubMed: 17631502]

[18]. Morrison JF. Kinetics of the reversible inhibition of enzyme-catalysed reactions by tight-binding inhibitors. Biochim Biophys Acta. 1969;185(2):269–286. [PubMed: 4980133]

[19]. Otwinowski Z, Minor W. Processing of X-ray diffraction data collected in oscillation mode. Methods Enzymol. 1997;276:307–326.

[20]. McCoy AJ. Solving structures of protein complexes by molecular replacement with Phaser. Acta Crystallogr D Biol Crystallogr. 2007;63(1):32–41. [PubMed: 17164524]

[21]. Afonine PV, Grosse-Kunstleve RW, Echols N, et al. Towards automated crystallographic structure refinement with phenix.refine. Acta Crystallogr D Biol Crystallogr. 2012;68(4):352–367. [PubMed: 22505256]

[22]. Emsley P, Lohkamp B, Scott WG, Cowtan K. Features and development of Coot. Acta Crystallogr D Biol Crystallogr. 2010;66(4):486–501. [PubMed: 20383002]

[23]. Chen VB, Arendall WB, Headd JJ, et al. MolProbity: all-atom structure validation for macromolecular crystallography. Acta Crystallogr D Biol Crystallogr. 2010;66(1): 12–21. [PubMed: 20057044]

[24]. Griffith EC, Zhao Y, Singh AP, et al. Ureadepsipeptides as ClpP Activators. Acs Infect Dis. 2019;5(11):1915–1925. [PubMed: 31588734]

[25]. North EJ, Scherman MS, Bruhn DF, et al. Design, synthesis and anti-tuberculosis activity of 1-adamantyl-3-heteroaryl ureas with improved in vitro pharmacokinetic properties. Bioorg Med Chem. 2013;21(9):2587–2599. [PubMed: 23498915]

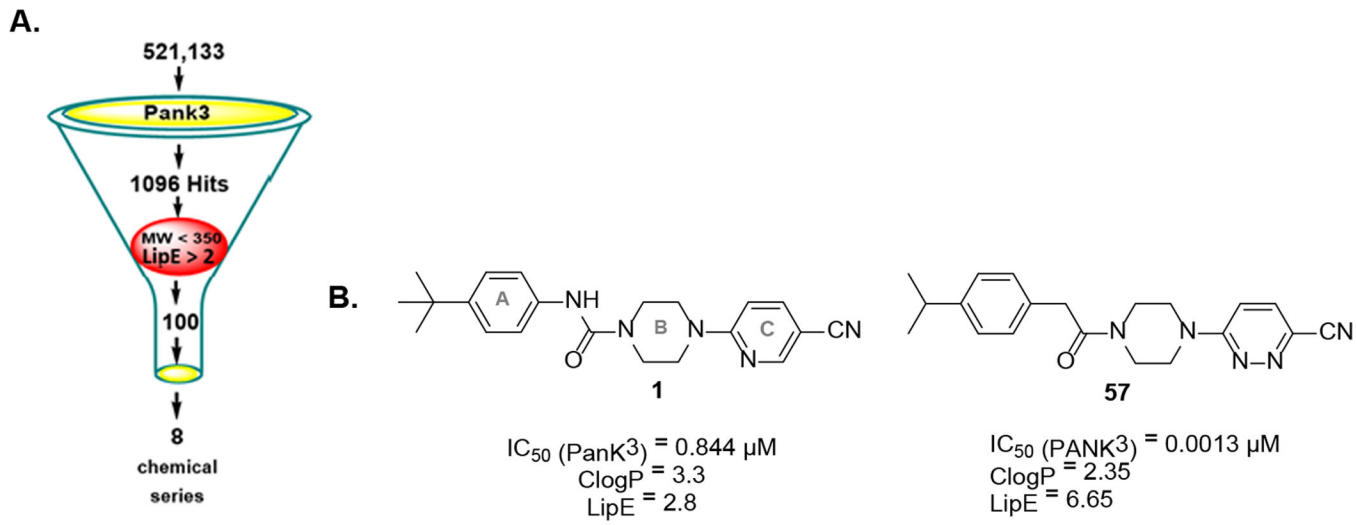

Figure 1.

A. Process of hit-triage using MW (<350) and LipE (>2) leading to 8 chemotypes. B. Chemical structure of screening hit (1) with piperazine ureas scaffold with ring labeling and optimized lead 57.

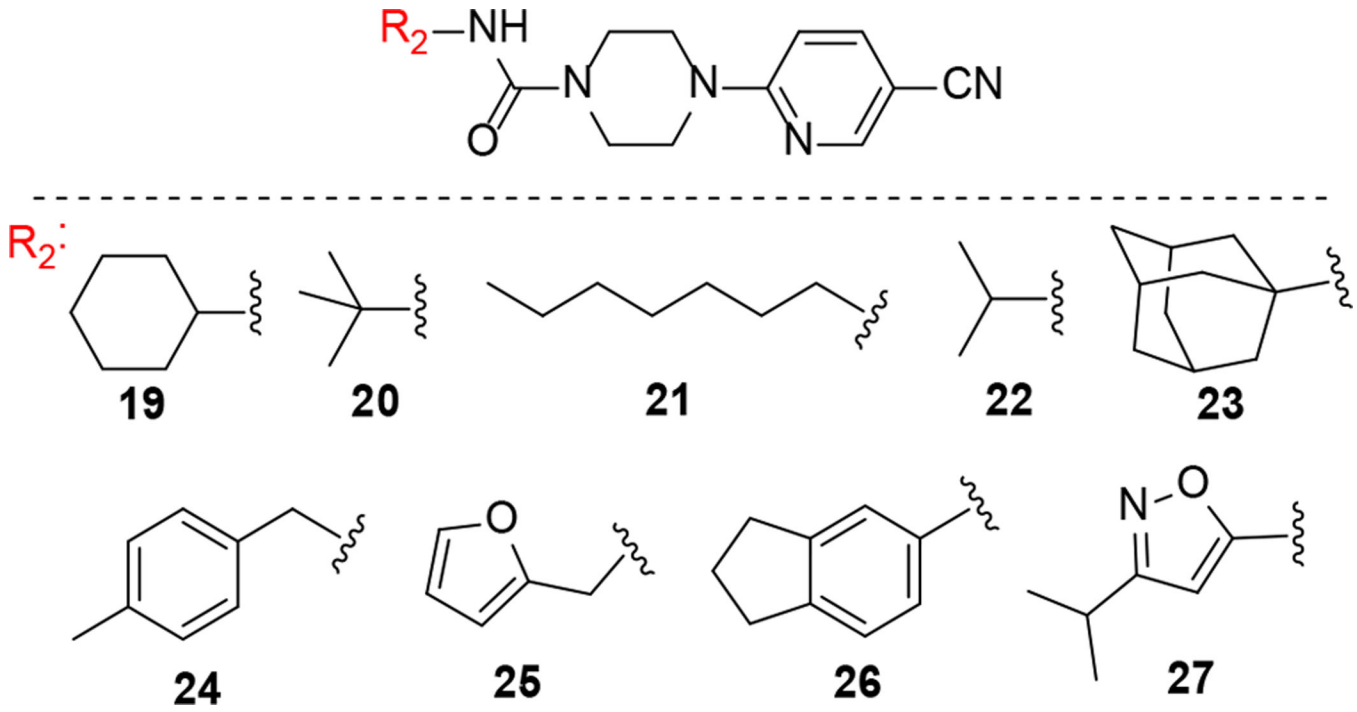

Figure 2.

Replacement of aniline ring with aliphatic and aromatic substituents. All these compounds (19–26) showed no activity (IC_{50} > 10 μM).

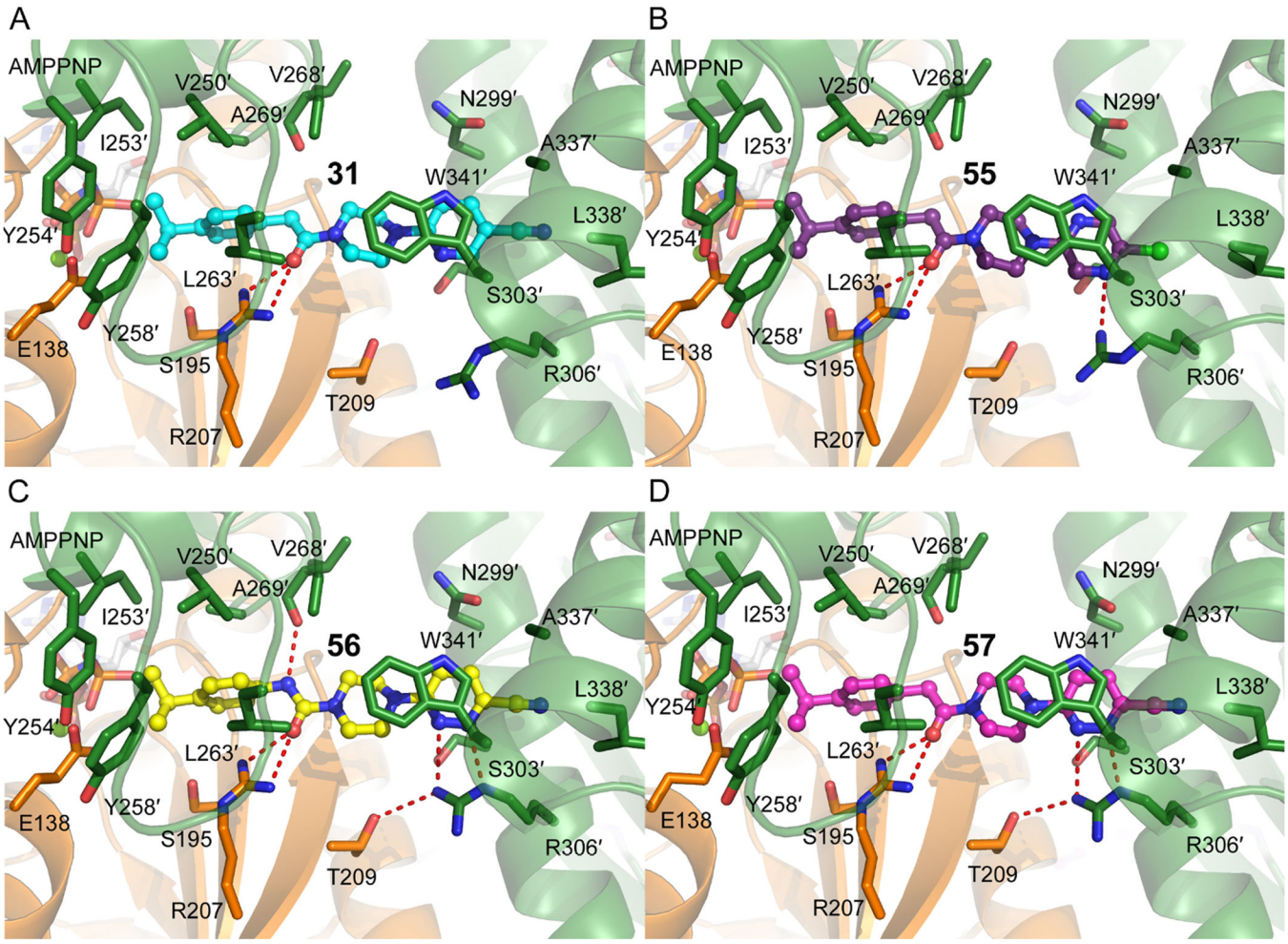

Figure 3.

Crystal structures of PANK3 in complex with 4 inhibitors. A. Compound **31** (cyan carbons) (PDB 6X4J); B. Compound **55** (purple carbons) (PDB 6X4L); C. Compound **56** (yellow carbons) (PDB 6X4K); D. Compound **57** (PZ-2891, magenta carbons) (PDB 6B3V). The views are identical in each figure. Monomer A (that contains the bound AMPPNP) is colored orange and monomer B (residues indicated with a prime) is colored green.

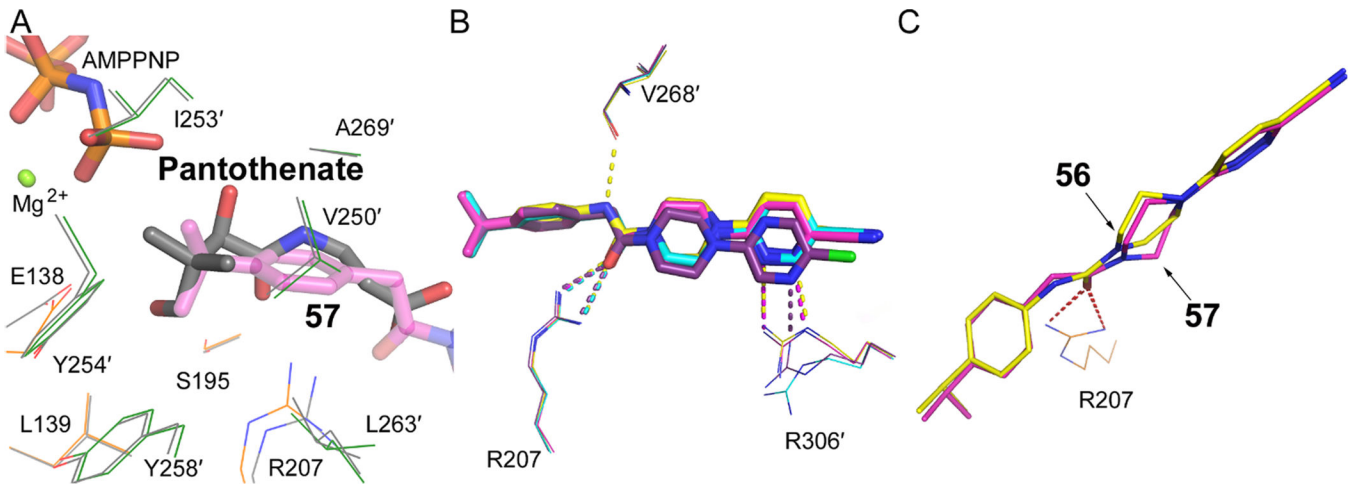

Figure 4.

Details of the key compound interactions. **A.** comparison of the Ring A isopropyl motif with pantothenate *gem*-dimethyl group's binding position within the active site; **57** (pink) (PDB 6B3V) overlayed on the ATP:Mg^{2+}:pantothenate (grey) structure (PDB 5KPR). [16] **B.** Superposition of the 4 compounds showing the displacements of rings B and C, and the interactions with Val268′, Arg207 and Arg306′. Compound **31** (cyan carbons); compound **55** (purple carbons)**; c**ompound **56** (yellow carbons); compound **57** (PZ-2891, magenta carbons). **C.** Distortion of ring B in **56** compared to **57**.

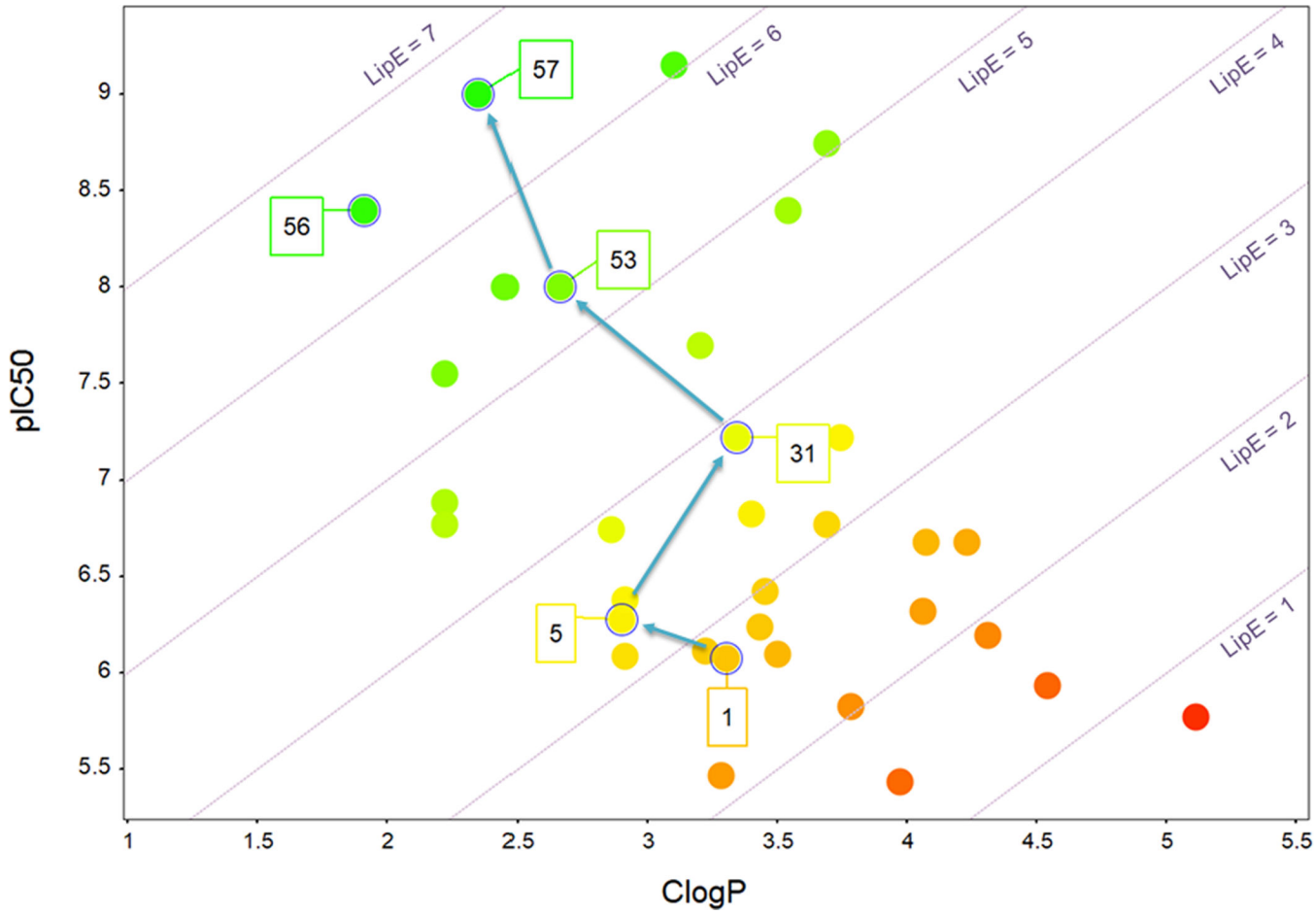

Figure 5.

Plot of clogP vs pIC_{50} showing optimization of HTS-hit (**1**) guided by LipE and eventually leading to lead **57**.

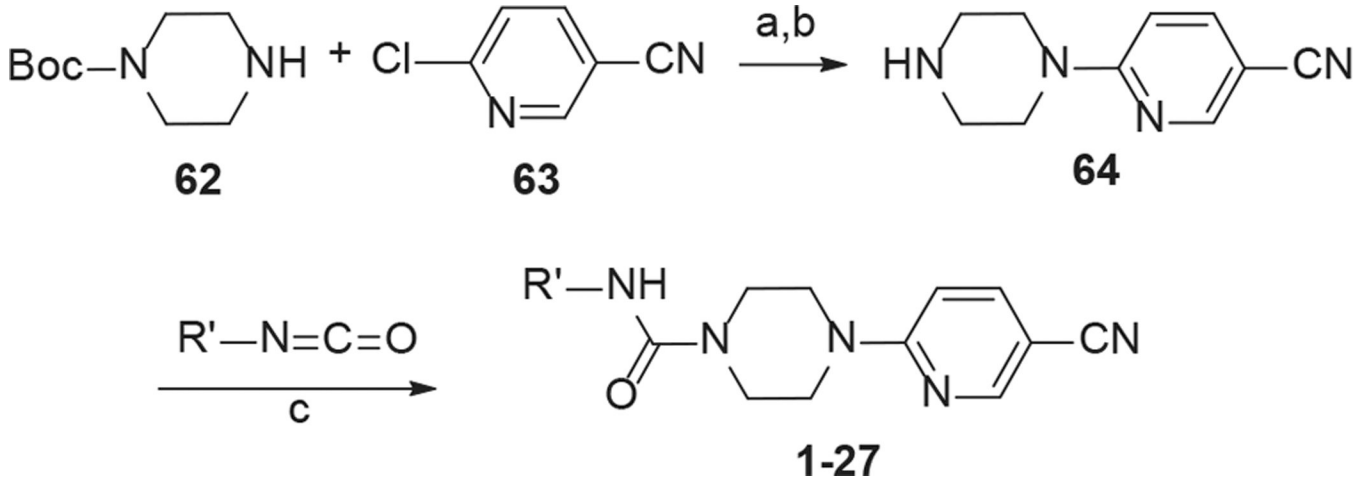

Scheme 1.

Synthesis of analogs **1**–**27**. *Reaction Conditions:* (a) Et_3N, CH_3CN, 160 °C, 30 min, microwave; (b) TFA-CH_2Cl_2 (1:1), rt, 1 h; (c) R'NCO (1.1 eq), Et_2O or CH_2Cl_2, Et_3N, rt, 3 h.

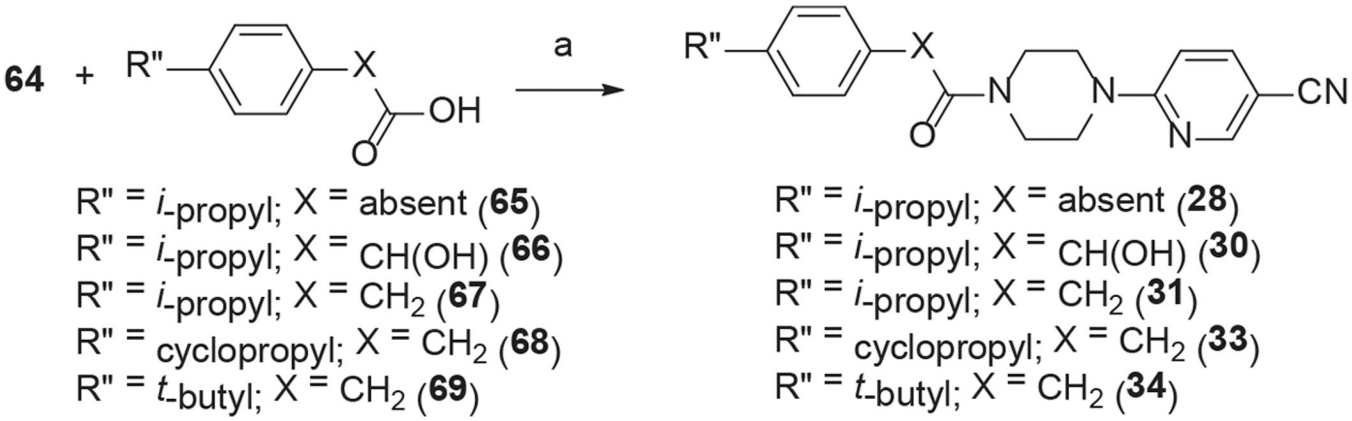

Scheme 2.

Synthesis of analogs **28, 30, 31, 33 and 34**. *Reaction Conditions:* (a) 6-(piperazin-1-yl)nicotinonitrile (**64**) (1 eq), acid (1.1 eq), HATU (1.1 eq), DIPEA (5 eq), CH_2Cl_2, rt, overnight.

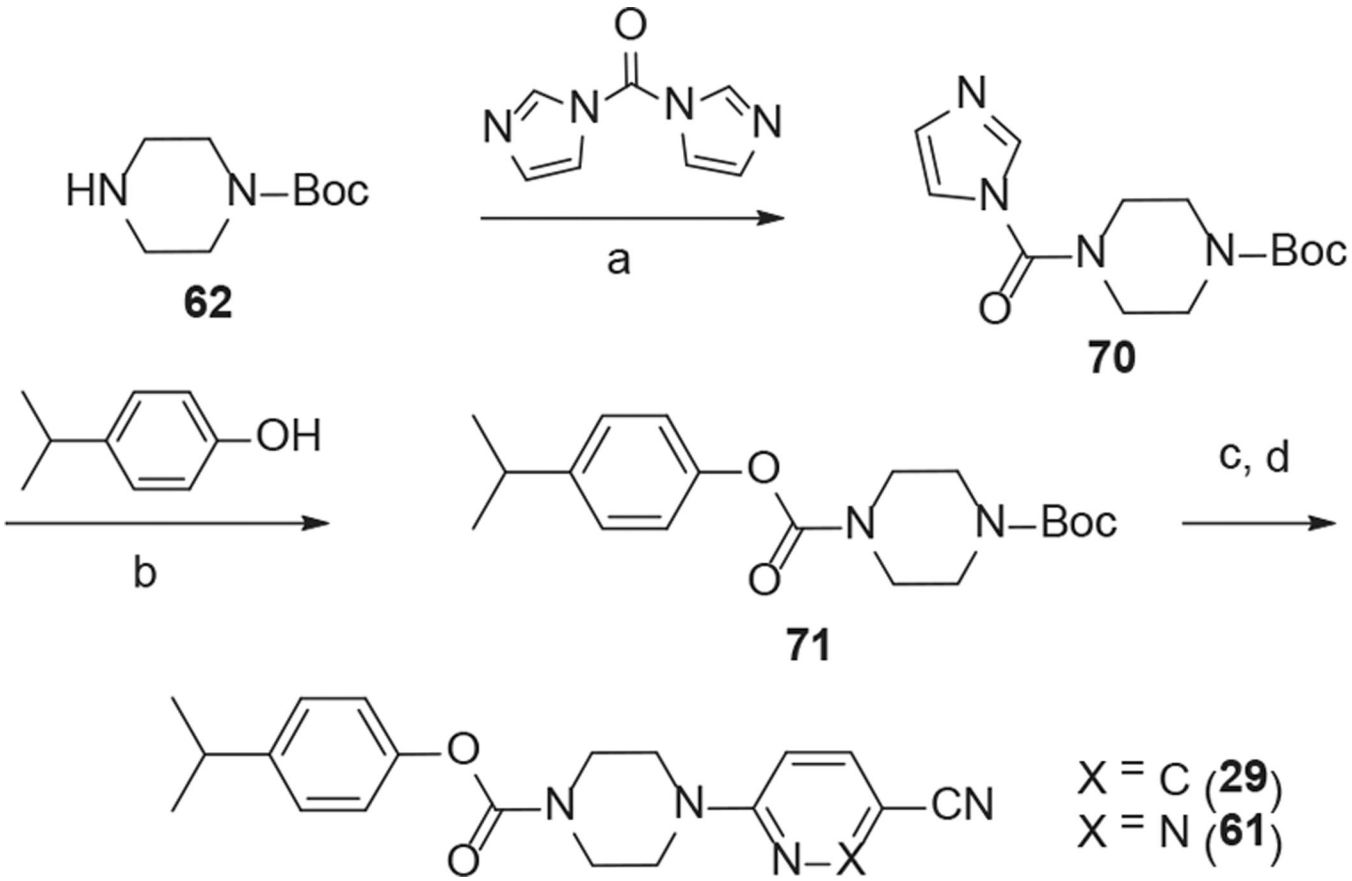

Scheme 3.

Synthesis of analogs **29** and **61**. *Reaction Conditions:* (a) CDI (2 eq), CH_2Cl_2, rt, overnight; (b) isopropylphenol (2 eq), Et_3N (5 eq), Cs_2CO_3 (2 eq), acetonitrile, 70 °C, 3–4 h; (c) TFA-CH_2Cl_2 (1:1), rt, 2 h; (d) 6-chloronicotinonitrile or 6-chloropyridazine-3-carbonitrile (1.1 eq), Et_3N (2 eq), acetonitrile, 160 °C, 30 min.

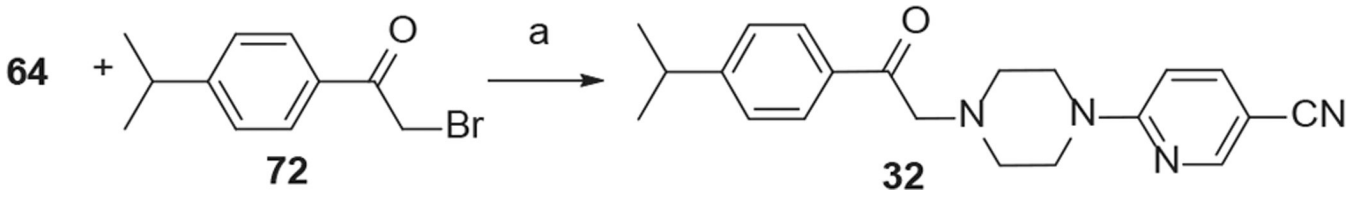

Scheme 4.

Synthesis of analogs **32**. *Reaction Conditions:* (a) 6-(piperazin-1-yl) nicotinonitrile (1 eq), 2-bromo-1-(4-isopropylphenyl)ethanone (1 eq), DIPEA (1 eq), CH_2Cl_2, rt, 3 h.

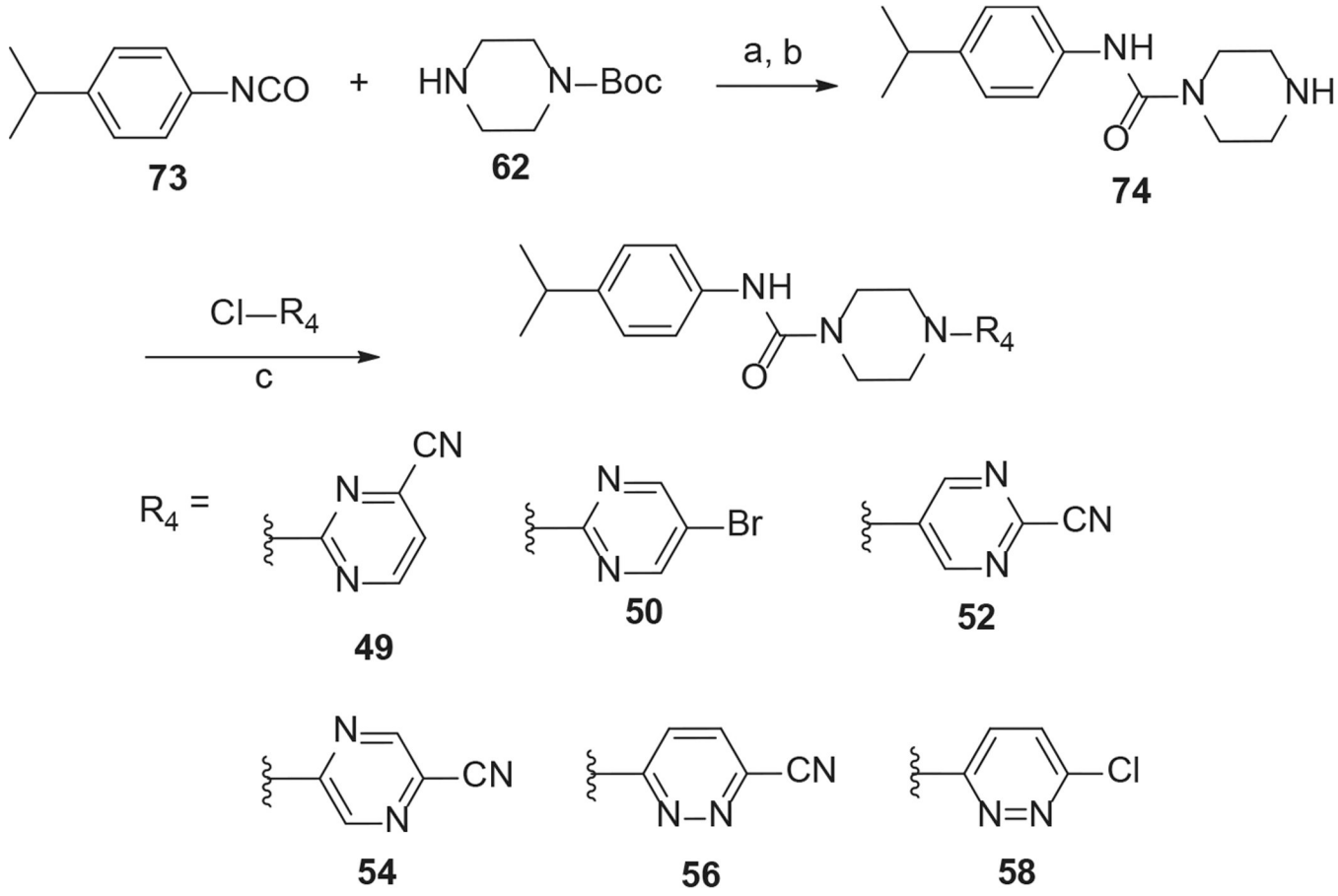

Scheme 5.

Synthesis of analogs **49**, **50**, **52, 54**, **56** and **58**. *Reaction Conditions:* (a) 1-isocyanato-4-isopropylbenzene (1.1 eq), Et_2O, rt, 3 h; (b) TFA-CH_2Cl_2 (1:1), rt, 1 h; (c) 6-chloronicotinonitrile (1.1 eq), Et_3N (2 eq), acetonitrile, MW, 160 °C, 30 min.

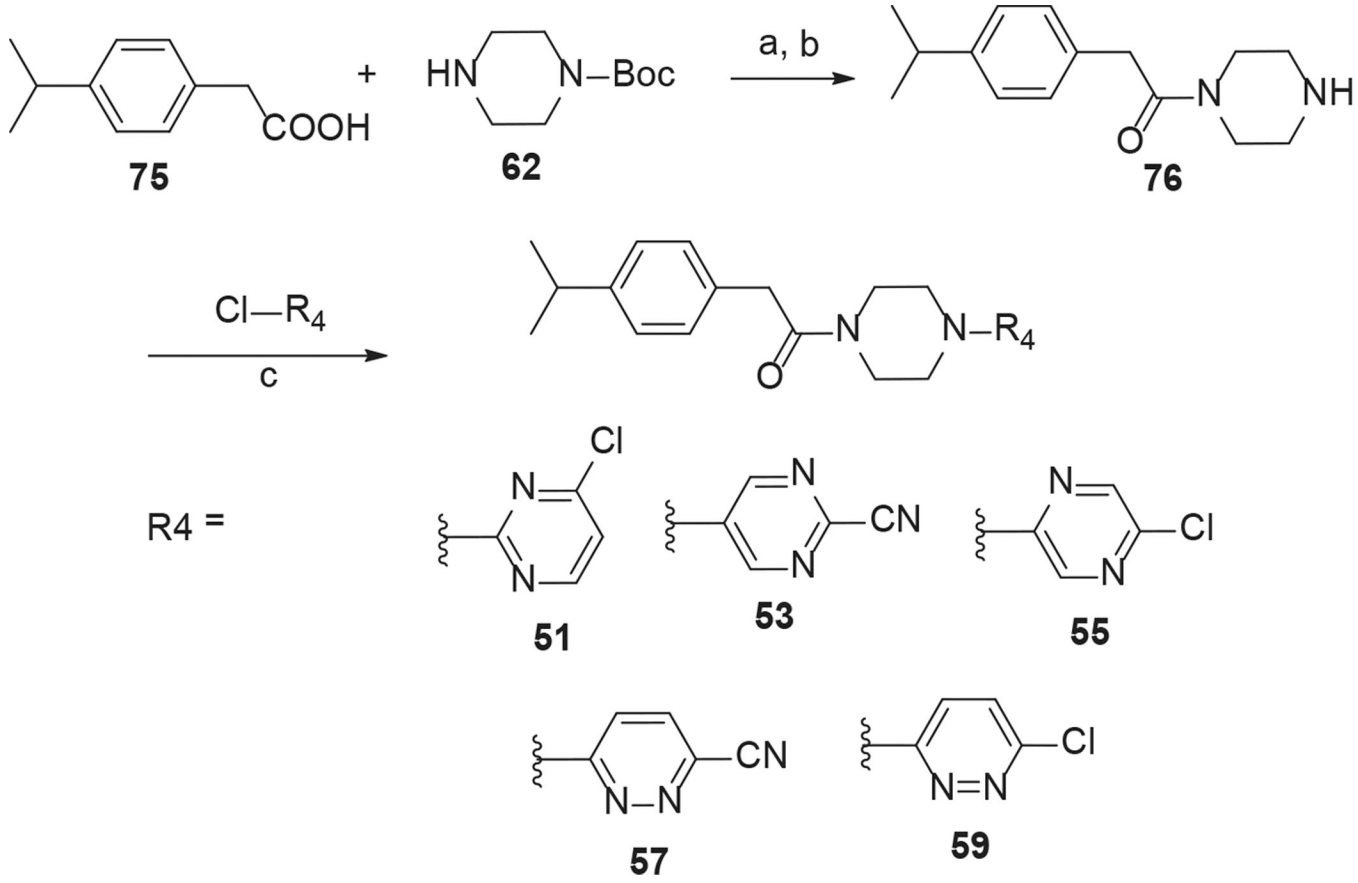

Scheme 6.

Synthesis of analogs **51**, **53**, **55**, **57** and **59**. *Reaction Conditions:* (a) HATU (1.1 eq), DIPEA (5 eq), CH_2Cl_2, rt, overnight; (b) TFA-CH_2Cl_2 (1:1), rt, 1 h; (c) 6-chloronicotinonitrile (1.1 eq), Et_3N (2 eq), acetonitrile, MW, 160 °C, 30 min.

Table 1

Substitutions on the aniline ring.

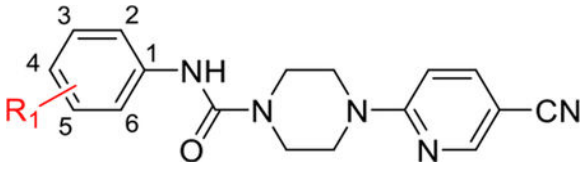

Compd	R_1	PANK3 IC_{50} (μm)	ClogP[a]	LipE[b]
1	4-*t*-Butyl	0.51 ± 0.05	3.30	2.80
2	H	>10	1.48	–
3	4-Ethyl	>10	2.50	–
4	4-*n*-Pentyl	>10	4.10	–
5	4-*i*-Propyl	0.64 ± 0.11	2.90	3.37
6	2-*i*-Pr, 6-Me	>10	2.03	–
7	4-*i*-Butyl	0.49 ± 0.09	3.43	2.80
8	4-*n*-Butyl	>10	3.56	–
9	2-Me, 4-*n*-Butyl	1.2 ± 0.22	3.50	2.59
10	4-OCH_3	>10	1.58	–
11	4-OCF_3	>10	2.69	–
12	4-$(CH_3)_2N$	>10	1.64	–
13	4-$COCH_3$	>10	1.47	–
14	4-Br	>10	2.64	–
15	4-Cl	>10	2.49	–
16	3-Cl, 4-Cl	>10	3.19	–
17	4-CN	>10	1.61	–
18	4-CF_3	>10	2.89	–

[a] LogP calculated by Chemdraw Professional 17.1

[b] IC_{50} values are reported as the mean. [b] LipE = pIC_{50} − ClogP.

Table 2

Effect of Variation of the Urea Linker.

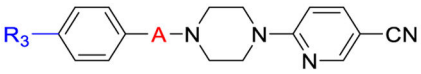

Compd#	A	R_3	PANK3 IC_{50} (μM)	ClogP	LipE
5			0.64 ± 0.11	2.90	3.21
28			>10	2.87	–
29			0.42 ± 0.07	3.45	2.97
30			0.99 ± 0.14	3.22	2.89
31			0.06 ± 0.004	3.34	3.60
32			>10	3.68	–
33			0.2 ± 0.015	2.86	3.88
34			0.06 ± 0.003	3.74	3.48

Table 3

Optimization of nicotinonitrile side chain.

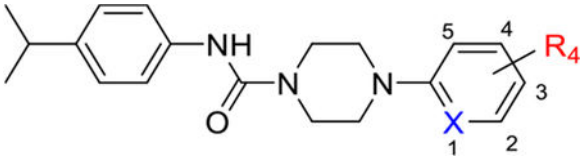

Compd #	X	R_4	PANK3 IC_{50} (μM)	ClogP	LipE
35	N	H	5.3 ± 0.76	3.28	2.18
36	N	3-CH_3	2.3 ± 0.27	3.78	2.04
37	N	3-NH_2	>10	2.95	–
38	N	5-CN	1.1 ± 0.11	2.91	3.17
39	N	4-CN	0.23 ± 0.03	2.91	3.46
40	N	3-NO_2	0.02 ± 0.004	3.20	4.49
41	N	3-CF_3	0.77 ± 0.14	4.31	1.88
42	N	3-Br	0.22 ± 0.04	4.23	2.44
43	N	3-Cl	0.22 ± 0.03	4.07	2.60
44	C	3-$COCH_3$	3.3 ± 0.36	3.97	1.46
45	C	3-F	1.8 ± 0.22	4.54	1.39
46	C	2-Cl	1.7 ± 0.21	5.11	0.65
47	C	3,4-di-Cl	1.4 ± 0.4	5.76	–
48	C	3-CN	0.58 ± 0.08	4.06	2.25

Table 4

Exploration of the heterocyclic aromatic ring.

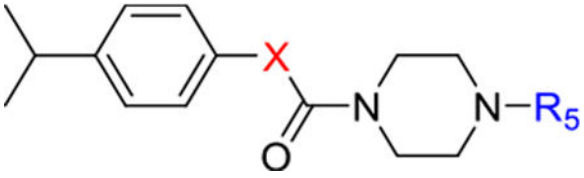

Compd #	X	R_5	PANK IC_{50} (μm)	ClogP	LipE
49	NH	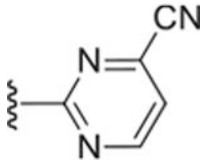	0.14 ± 0.015	2.22	4.66
50	NH	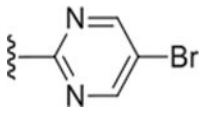	0.16 ± 0.012	3.40	3.42
51	CH_2	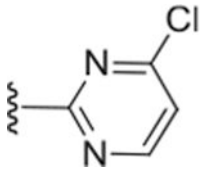	0.27 ± 0.054	3.69	3.07
52	NH	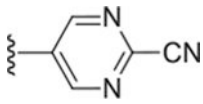	0.17 ± 0.017	2.22	4.54
53	CH_2	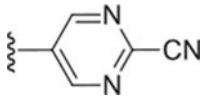	0.01 ± 0.001	2.66	5.34
54	NH	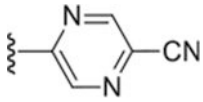	0.029 ± 0.004	2.22	5.33
55	CH_2	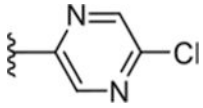	0.0018 ± 0.0002	3.69	5.05
56	NH	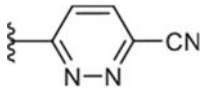	0.004 ± 0.0006	1.91	6.48

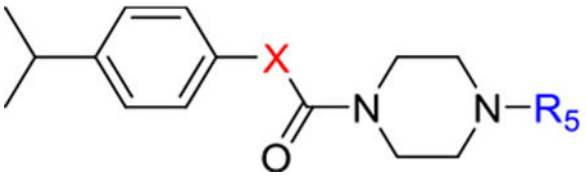

Compd #	X	R_5	PANK IC_{50} (μm)	ClogP	LipE
57	CH_2	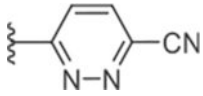	0.001 ± 0.0001	2.35	6.65
58	NH	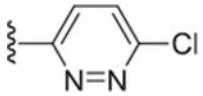	0.0007 ± 0.0001	3.10	6.05
59	CH_2	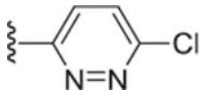	0.0004 ± 0.0002	3.54	5.85
60	CO	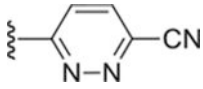	>10	1.75	–
61	O	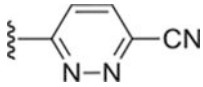	0.01 ± 0.001	2.45	5.55

Table 5

In Vitro ADME Profile of **1**, **56** and **57**.

	1	**56**	**57***
Solubility at pH = 7.4 (μM)	1.4	5.5	23
PAMPA (1×10^{-6} cm/s)	1232	316	413
Caco2 Permeability (nm/s)			
A/B	161	243	302
Plasma Protein Binding (%)			
mouse	99	92	92
rat	98	89	91
human	99	92	93
Metabolic Stability ($T_{1/2}$, min)			
mouse	16	113	8
rat	31	294	47
human	8	64	7
Plasma Stability ($T_{1/2}$, h)	>48	>48	>48

*previously determined.[8]